İSTANBUL TECHNICAL UNIVERSITY ★ INSTITUTE OF SCIENCE AND TECHNOLOGY

THEORETICAL INVESTIGATION of CH/π INTERACTIONS in NITROGEN CONTAINING AROMATIC SYSTEMS by POST-HF and DFT-SAPT METHODS

M.Sc. Thesis by
Berkay SÜTAY

Department : Chemistry

Programme : Chemistry

JUNE 2010

İSTANBUL TECHNICAL UNIVERSITY ★ INSTITUTE OF SCIENCE AND TECHNOLOGY

THEORETICAL INVESTIGATION of CH/π INTERACTIONS in NITROGEN CONTAINING AROMATIC SYSTEMS by POST-HF and DFT-SAPT METHODS

M.Sc. Thesis by
Berkay SÜTAY
(509081241)

Date of submission : 07 May 2010
Date of defence examination: 11 June 2010

Supervisor : Prof. Dr. Mine YURTSEVER (ITU)
Members of the Examining Committee : Assoc. Prof. Dr. Nurcan TÜZÜN (ITU)
Assist. Prof. Dr. Adem TEKİN (ITU)

JUNE 2010

İSTANBUL TEKNİK ÜNİVERSİTESİ ★ FEN BİLİMLERİ ENSTİTÜSÜ

NİTROJEN İÇEREN AROMATİK SİSTEMLERDEKİ CH/π ETKİLEŞİMLERİNİN GELİŞMİŞ-HF ve DFT-SAPT YÖNTEMLERİYLE TEORİK OLARAK İNCELENMESİ

YÜKSEK LİSANS TEZİ

Berkay SÜTAY
(509081241)

Tezin Enstitüye Verildiği Tarih : 07 Mayıs 2010
Tezin Savunulduğu Tarih : 11 Haziran 2010

Tez Danışmanı : Prof. Dr. Mine YURTSEVER (İTÜ)
Diğer Jüri Üyeleri : Doç. Dr. Nurcan TÜZÜN (İTÜ)
Yrd. Doç. Dr. Adem TEKİN (İTÜ)

HAZİRAN 2010

I Remember the First

Time That I Saw The Proton Map of

Formaldehyde …

PREFACE

The second time that i have the chance to make something scientific as a person who believes that the science is universal and tries to improve himself in this way. So that, i wanted to produce something that bears some traces of my scientific point of view. The insufficient construction of science in Turkey is perceived mostly in Chemistry (=Physics), however the whole world has the same problem as a vicious cycle. That's why the chemistry could not be improved theoretically in our country, that has caused the construction of this area on a ground in lack of resistance. All these became the reasons which are responsible for directing me to study in Theoretical Chemistry area – although not prefering to use this name, because the whole of chemistry is theoretical.

In this master thesis, in which we have started our studies directed towards to such kind of aim, we profited from Quantum Mechanics and of course Mathematics as the glorious languages of our nature.

I wish to thank Prof. Dr. Mine YURTSEVER who is my teacher, my advisor and the head of my new family. I always felt the taste of working freely with her, freely but with perfect confidence. If this study is a qualified one, it is of that she supplied the perfect conditions to work for me. Thanks for her kindness and reliance on me that is what a student always needs.

I am very grateful to Yrd. Doç. Dr. Adem TEKİN for his kind interest he showed in this work. He was kind enough in doing all calculations with me and supplied to grow myself practically beyond chemistry and thanks for all that he taught me. He always made me feel so close to him beyond a teacher.

Several people to whom i had asked their advice, have kindly given me their criticism; among them i should like to mention Erol Yıldırım for having suggestions to me and endless help when i need and Songül Güryel for her worthy help and lovely friendship.

I am grateful to all those in my second family that made me feel as a part of them from the very very beginning.

I hope this study will be one of my many work in future...

June, 2010 **Berkay Sütay**

TABLE OF CONTENTS

Page

ABBREVIATIONS

IR :Infrared Spectroscopy
NMR :Nuclear Magnetic Resonance
XRD :X-Ray Diffraction
HF :Hartree-Fock Theory
CC :Coupled Cluster Theory
CI :Configuration-Interaction Theory
BD :Brueckner Doubles Theory
MPN :Moeller-Plesset Perturbation Theory
MET :Many Electron Theory
IEPA :Independent Electron Pair Approximation
CEPA :Coupled Electron Pair Approximation
CPMET :Coupled Pair Many Electron Theory
L-CC :Linear Coupled Cluster Theory
MCSCF :Multiconfigurational Self Consistent Field Theory
CASSCF :Complete Active Space Self Consistent Field Theory
GVB :Generalized Valence Bond Theory
RI :Resolution of Identity Integral Approximation
SCS :Spin Component Scaling
DFT :Density Functional Theory
DFT-D :Density Functional Theory with empirical dispersion correction
SAPT :Symmetry Adapted Perturbation Theory
PES :Potential Energy Surface
BSSE :Basis Set Superposition Error
CP :Counterpoise Correction
QED :Quantum Electrodynamics
PEC :Potential Energy Curve

LIST OF TABLES

Page

LIST OF FIGURES

Page

LIST OF SYMBOLS

E	**:** Energy of the System
∆E	**:** Interaction energy
H	**:** Hamiltonian Operator
N	**:** Normalization Constant
Ψ	**:** Wavefunction
T	**:** Tensor operator
$\mathbf{E_{corr}}$	**:** Correlation energy
Θ	**:** Quadrupole moment
μ	**:** Dipole moment
α	**:** Polarizability
β	**:** Hyperpolarizability
$\hat{u}_{ij}$	**:** Two electron correlation function
Φo	**:** HF determinant
X	**:** Correlation Function
$\tilde{\nu}$	**:** Wavenumber
π	**:** Pi bond

THEORETICAL INVESTIGATION of CH/π INTERACTIONS in NITROGEN CONTAINING AROMATIC SYSTEMS by POST-HF and DFT-SAPT METHODS

SUMMARY

There is a weak intermolecular interaction that occurs in the clusters of aromatic systems including at least one aromatic compound which is a combination of several kind of interactions as NH/π, CH/π, OH/π, SH/π, π/π, N/π, O/π, S/π, etc. In this study, the interactions in the pyrazine and triazine dimers were investigated for different orientations of monomers and the conformers were treated by CCSD(T) as the most accurate computational method. Basis sets were chosen as aug-cc-pVDZ and aug-cc-pVTZ as two of the largest ones. DFT-D, MP2, SCS-MP2 and DFT-SAPT calculations have also been performed in comparison to CCSD(T) results to test the performances of these methods in such kind of weak intermolecular interactions. The potential energy curves of different conformations have been treated with respect to center of mass distances. This kind of potential energy curves were found important to figure out which computational method is the most suitable one to perform a molecular dynamics simulation to enlighten the crystalization processes of pyrazine and triazine. DFT-SAPT components were also been computed to explain which interaction has the dominant effect in total interaction potential. The relativistic corrections had also been performed in the sense of relativistic quantum chemistry to test how much these corrections are important in such kind of weak interactions.

NİTROJEN İÇEREN AROMATİK SİSTEMLERDEKİ CH/π ETKİLEŞİMLERİNİN GELİŞMİŞ-HF ve DFT-SAPT YÖNTEMLERİYLE TEORİK OLARAK İNCELENMESİ

ÖZET

Aromatik sistemlerin dimer, trimer, tetramer, vb küme yapılarında ya da en az bir aromatik sistem içeren molekül kümelerinde NH/π, CH/π, OH/π, SH/π, π/π, N/π, O/π, S/π, vb., zayıf moleküller arası etkileşimler mevcuttur. Bu çalışmada pirazin ve triazin dimerlerindeki zayıf etkileşimler ele alınmıştır. Bu amaçla farklı dimerik yapılar için etkileşim enerjileri, bu aşırı hassas etkileşimleri yüksek doğrulukla elde etmek üzere CCSD(T) yöntemi ile aug-cc-pVDZ ve aug-cc-pVTZ temel setlerinde hesaplanmıştır. Bu zayıf etkileşimlerde MP2, SCS-MP2, DFT-D ve DFT-SAPT yöntemlerinin performanslarını görebilmek üzere CCSD(T) sonuçlarıyla karşılaştırmalı olarak bu metotlarla da aynı hesaplar yinelenmiştir. Farklı kütle merkezi koordinatları için incelenen konformerlerin potansiyel enerji eğrileri elde edilmiştir. Bu tip potansiyel enerji eğrileri, kristalleşme süreçlerini aydınlatacak moleküler dinamik simülasyonlarının yapılmasında hangi metodun en uygun olduğunu anlamamızı sağlaması açısından önemli bulunmuştur. Toplam etkileşimde hanig etkileşim türünün baskın nitelikte olduğunu anlamak için DFT-SAPT yöntemi ile enerji bileşenleri hesaplanmıştır. Ayrıca rölativistik kuantum mekaniğinden gelen düzeltmeler de hesaplanmış ve rölativistik kuantum kimyası açısından bu etkileşimlere görelilikten gelen katkıların ne derece önemli olduğu sınanmıştır.

1. INTRODUCTION

1.1 Historical Background (Discovery and importance)

The earliest references to concepts that would be termed hydrogen bonds occur in the German literature; Werner (1902) and Hantzsch (1910) used the term "Nebenvalentz (secondary valence)" to describe the binding in ammonia salts. Then in 1910s, it is investigated that in organic chemistry in the process of explaining the reactivities of carbonyl and alcohol compounds. Moore and Winmill (1912) called it "weak union" and then, Latimer and Rodebush (1920) made the first electrostatic definition of hydrogen bond as "a free pair of electrons on one water molecule might be able to exert sufficient force on a hydrogen atom on another water molecule to bind two molecules together" (1).

Before the advent of quantum mechanics, the hydrogen bonds were thought to be purely electrostatic; e.g. the oxygen atom in a water molecule has a partial negative charge in contrast to positively charged hydrogens. But in 1935, Linus Pauling (known as the father of the quantum chemistry) suggested that quantum mechanics governs the hydrogen bonds between water molecules as well as the covalent bonds inside the molecules (2). Pauling, who used the term "Hydrogen bond" first, handled this concept as a manifestation of the fact that electrons in water obey the bizarre laws of quantum mechanics!

In 1959, H/π type hydrogen bond interactions were first reported by Oki and Iwamura from the measurements of the IR spectra of N-Benzylaniline and its derivatives, that was NH/π interaction (3). In 1960, these aromatic hydrogen bonds were suggested to be investigated in the book of Pimentel, "Do aromatics form hydrogen bonds?" (4). In 1960s and 1970s, the effect of these kind of interactions on the IR spectra of some chemical species were investigated (6,7,8,9,10,11). In 1986, Perutz reported the NH/π interaction in the hemaeoglobin-drug complex (12). In 1990s, these interactions became easily observable in detail by the recently

developed supersonic jet spectral studies and also the UV-IR double resonance spectra (13,14).

"Aromatic hydrogen bonding" as a special type of XH/π hydrogen bonds plays a dominant role in many forefront areas of chemistry from molecular biology to material design. It is expected to play a significant role in molecular associations due to making an important contribution to the stabilizing enthalpy (15). These weak interactions play vital roles in processes such as protein-ligand recognition, enzymatic activitiy, packing of aromatic molecules within molecular crystals, antigen-antibody binding, base-base interaction in DNA and the determination of three dimensional structures of nucleic acids and proteins; furtherly it is a stabilizing factor in β-sheets, peptide β-hairpins, helix termini, proline residues in protein structures, packing of transmembrane helices, collagen, DNA, etc (16). Since these interactions can occur more frequently than regular hydrogen bonds albeit being so weak in strength, they may well contribute to the properties of the system. Especially, in protein structures, it is interesting that a larger number of CH/π interactions (almost a few hundreds) can be explained in terms of the larger abundance of CH groups (17).

1.2 Intermolecular Forces

Atoms, molecules, ions, etc. as the fundamental components of the matter constitutes the solids, liquids, gases by the equilibrium state between attraction and repulsion forces which are called as "intermolecular interactions". The Hamiltonian of the thermodynamic system contains the potential energy function of the interaction between the particles and it is simply a function of internuclear distances and orientations of systems in space;

$$V(r) = V_{tr} + V_{rot} + V_{vib} + V_{el} + V_{rest} + V_{intermol} \qquad \textbf{(1.1)}$$

In solids, the molecules generally do not undergo translation or rotation.

Intermolecular forces produce a potential energy well similar to an atom or molecule due to it is a Born-Oppenheimer (BO) energy too, changing with the distance as different solutions of Schrödinger equation at different points. Both chemical bonds

and intermolecular interactions are the BO energies and also, the intermolecular interactions are somewhat small in comparison with the chemical bonds. Lennard-Jones potential is an approximation to the BO energy of interacting systems. There are also some other approximations different from Lennard-Jones which is the most famous one.

Intermolecular forces can be classfied in such a manner (18,19):

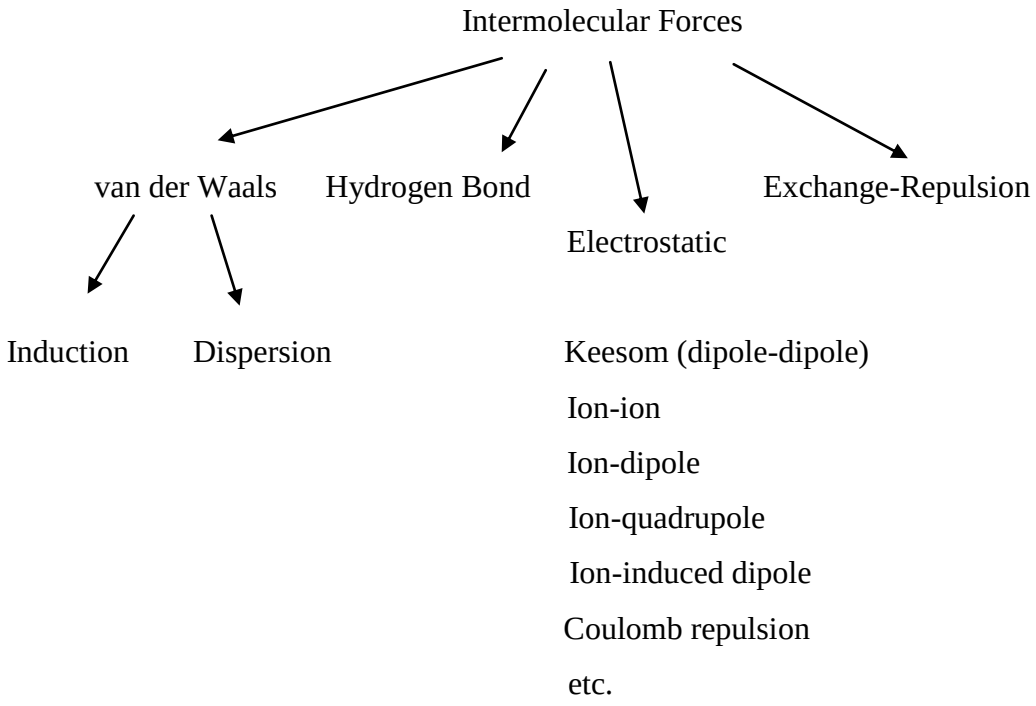

One may also classify these interactions in terms of their short or long range properties:

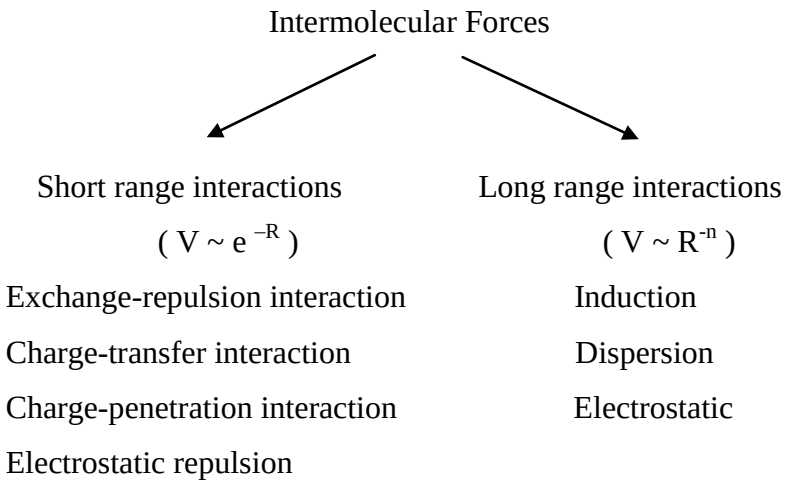

Short range interactions exhibit exponential decreasing ($e^{-\alpha R}$) which are generally repulsive and isotropic while long range ones are anisotropic, generally attractive except from electrostatic repulsion and exhibit R^{-n} decreasing with the increasing distance.

In the dispersion interaction, the attraction near the minimum is due partly to the "distortion" of orbitals, but especially at large distances, it arises from simultaneous excitations in both systems. The distortion effect is automatically included in a Hartree-Fock orbital part on the SCF-MOs, for the composite system of the interacting atoms. In modern quantum theory, there is an overlap between the ground state atoms and also there is an overlap between any of the atomic excited states in contrast to modest London dispersion theory. It has been shown that, by Pitzer (20) , the dispersion energy is purely of electron correlation, thus one needs an extensive correlation theory to get the highest portion of the correlation energy as the dispersion interaction!

1.3 Hydrogen Bonding

Hydrogen bonds are traditionally defined as occuring between a donor hydrogen and an electronegative acceptor with lone pairs. A more general and comprehensive definition is that hydrogen bond can be viewed as a "*metric-dependent electrostatic scalar field*" between two or more intermolecular bonds. These bonds may occur between molecules as "intermolecularly" or within different parts of a single molecule as "intramolecularly" (21).

Classical hydrogen bonds are largely electrostatic in nature; so, other suitable sources of electron (without involving an electronegative atom) could also act as an acceptor group; such as pi bonds, aromatic rings, etc. Therefore, aromatic rings can interact with hydrogen donors and aromatic hydrogen bond occurs! For example, HF, HCl, H_2O, H_2S and NH_3 can make hydrogen bonds with benzene, pyridine, etc. This "aromatic hydrogen bonding" interactions are much lower than the classical hydrogen bond; approximately up to -10 kJ/mol (compared to -30 kJ/mol classical ones) (22). One may classify the hydrogen bonds (H-bonds) as in the figure below.

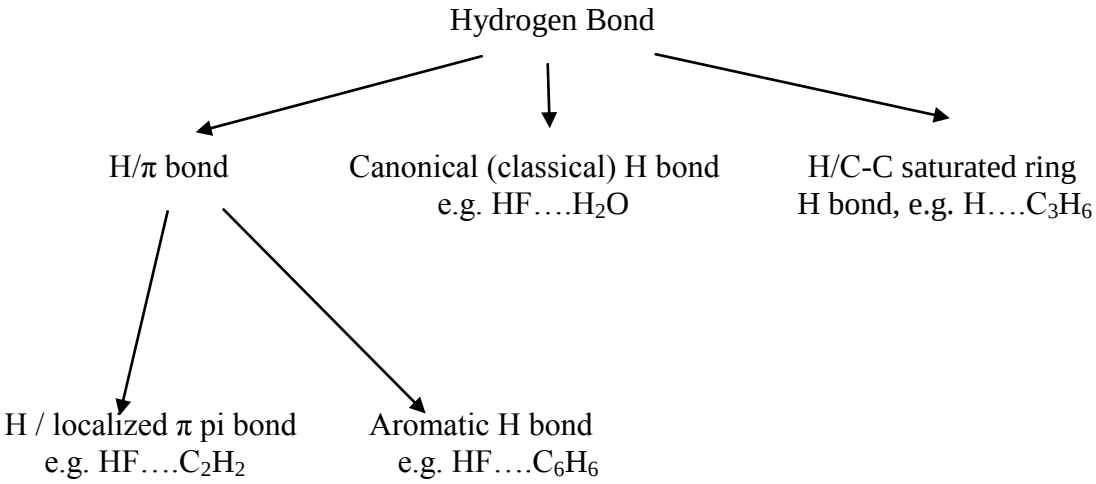

H-bonds are attractive, having internuclear distances from 2 Å up to 3,5 Å, anisotropic and can be mainly considered of "long range". Typically, it produces interatomic distances shorter than sum of vdW radii.

The H-bond potential energy function can be given as the sum of four main components (15);

$$E_{HB} = E_{elec} + E_{exc\text{-}rep} + E_{disp} + E_{ch\text{-}tr} \qquad (1.2)$$

where charge transfer energy is the induction energy! Charge-transfer is generally too small, sometimes can be neglected; it becomes important between similar molecules; e.g. pyrrole dimers, etc.; it is also important at small distances (R). Classical H-bond energies are typically 30 kJ/mol is comparable to that of weak covalent bonds (≈120 kJ/mol). It is the strongest interaction among the other intermolecular forces; it is responsible for the high boiling points of liquids and also causes a negative deviation from the Raoult's law.

1.4 Aromatic Hydrogen Bonding

Brinkley and Gupta (22) investigated the interaction on the 1-Hexanol/Toluene model system by IR experimental analysis. They found that the OH peak was broader and stronger, having less wavenumber ($\Delta\tilde{\nu} = 40$ cm^{-1}) for 1-Hexanol/toluene system in comparison to the case without toluene, Fig. 1.

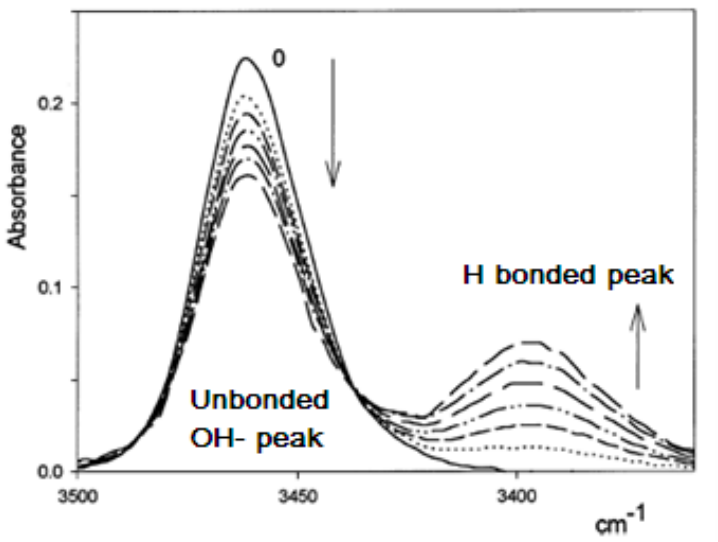

Figure 1 : IR spectrum of alcohol-toluene system

What was the reason for that situation? To answer this question, they performed a series of experiments to determine solute/solvent mol fraction ratios to compare the results with IR spectral results. They have found that % H-bonded alcohol concentration rises rather slowly with increasing aromatic compound concentration despite the large aromatic/alcohol ratio. That fact could lead to two hypotheses:

1. The H-bond between alcohol and aromatics is fairly weak!
2. The H-bond is affected by some steric factor!

By the experiments, the estimated aromatic H-bond energies are within -7 kJ/mol in comparison with the ethanol-ethanol (self alcohol system) value, -25 kJ/mol which is much higher than for aromatic H-bonds. Therefore, one may get the result that m-xylene has a stronger aromatic H-bond with ethanol than toluene. According to these lower energies, the equilibrium constant for self alcohol H-bonding is about 300 times that for aromatic ones; in other words, aromatic H-bonds are 300 times weaker than the alcohol self association. Nonetheless, these small energies cannot be negligible. In phase equilibria calculations, aromatic molecules often require adjustable binary parameters to fit the data, using theories that describe alkane mixtures! This is necessary; because thermodynamic effects of H-bonding are important in determining the phase behaviour in polar fluids. This H-bonding contributes significantly to the chemical potential (μ) of the molecules.

We know that the aromatic H-bond is weak in strength, and also they play an important role in stability; but why? Because, e.g. at room temperature, the amino-

benzene interaction energy is about -3 kcal/mol which is 5 times the room temperature thermal energy $E_{thermal}$ = 0,6 kcal/mol (for 300 ^{0}K) and can be expected to play a key role in stabilizing molecular interactions (12).

In aromatic systems, hydrogen tends to point toward the midpoint of the ring; namely to the centre; but it can also be pointed toward to only one of the pi bonds, not only toward to the centre of the ring and also, spectroscopic results have shown that not only one structure is possible for these interactions, more than one possible orientations can be equilibrium structures (23). A statistical analysis of the crystal structure database also confirmed that all different types of orientations exist in crystals (15), Fig.2.

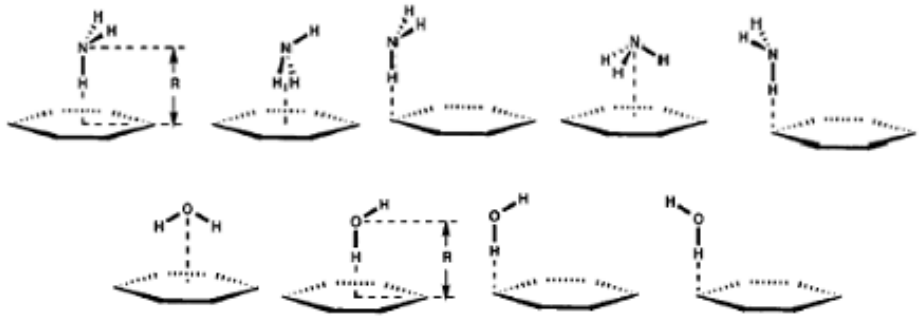

Figure 2 : The possible orientations for ammonia and water complexes of benzene

This also shows that the geometry of XH/π bonds is very flexible, allowing large displacement of the donor.

Optimum H/π bond lengths were determined within 2,1 Å for localized pi systems; but up to 3,7 Å from 2,1 Å for aromatics! Additionally, in the case of benzene, charge transfer and X-ray H...π distance informations indicate that XH/π hydrogen bonds for localized pi systems are stronger than the aromatic ones.

1.4.1 Aromatic Hydrogen Bond Potential Energy Function

Aromatic H-bonding interaction can be represented by the same potential energy function as the classical H-bond; the main difference is of different magnitudes of each component. Likewise a many electron system, if one writes down the energy expression as;

$$E = E_{HF} + E_{corr} = E_{el} + E_{exc\text{-}rep} + E_{ch\text{-}tr} + E_{disp} \quad \textbf{(1.3)}$$

in which the electrostatic, exchange-repulsion and charge transfer interactions are mainly of HF orbital part and the correlation part is responsible for the dispersion.

Electrostatic energy is calculated as an interaction between the distributed multipoles of isolated molecules. It has been shown that electrostatic energies strongly depend on the orientation of the complexes; so it is important in determining the relative stability of the complexes. It has also been reported that from simple model calculations, structures of molecular clusters are mainly determined by the exchange-repulsion and electrostatic interactions, the most appropriate geometry is the one that minimizes the exchange-repulsion. On the other hand, dispersion energy is responsible for the attraction as the largest contribution to the total interaction energy. However, dispersion interaction is larger than electrostatic energy. Although the electrostatic energy is not large and dispersion is important for the attraction in the XH/π interactions, the electrostatic interaction plays an important role in determining the magnitude (order of the energy) and the directionality of the XH / π interactions. Electron correlation greatly increases calculated interaction energies which indicates that the dispersion interaction is important for the attraction in these complexes.

The calculated interaction energies have strong orientation dependence even in a long intermolecular separation (R > 4,5 Å) . The orientation dependence is the same as that in a short separation which suggests that the directionality in both short and longe R distances, is controlled mainly by the electrostatic interaction which is of longe range. If short range interactions such as "charge transfer" are the major source of the directionality, this directionality should disappear in a long separation. Consequently, charge transfer is not essential for the attraction and directionality of XH / π interactions.

The aromatic H-bond interaction energies are approximately 1 - 4 kcal/mol (≈ 4 - 12 kJ/mol). The dispersion interaction has the largest contribution to total interaction energy while the electrostatic energy is important for the directionality and the structure. The order of the E_{total} values agrees with the electronegativity order of the proton donating atoms (C < N < O). This aggreement also indicates that the magnitude of the interactions is mainly governed by the electrostatic interaction; as

we know H-bonding is already causes from the electrostatic interaction in relative magnitude.

1.4.2 Comparison of Classical and Aromatic Hydrogen Bonds

Classical and aromatic H-bonds having the same potential energy expression with completely different components in order may be compared in the characteristic below (17):

Classical H-bond: Electrostatic > Exchange-repulsion > Dispersion

Aromatic H-bond: Dispersion > Exchange-repulsion ≈ Electrostatic

Generally, In the aromatic H-bonding case, the electrostatic contribution is too small for CH/π interactions which are mainly of dispersion; but is has larger part of the energy for OH and NH/π, etc. type interactions due to higher partial charges on N, O, etc. atoms. The model calculations have showed that, the dispersion energy is larger than almost 2 times of the electrostatic energy in absolute values.

1.4.3 Experimental Observation of Aromatic Hydrogen Bonds

Aromatic H-bonding interactions can be observed in five main types of experimental analysis techniques as; IR, Raman, MW, NMR spectroscopies and XRD. IR spectra have shown evidence of intra- and intermolecular aromatic H-bonding (Rozas). The IR shifts observed in NH, OH, etc. type stretching peaks give some information about aromatic H-bonding interaction energies. These interactions always cause to red shifts via the decreasing wavenumber of peaks for stretching modes. Jet FTIR and jet Raman spectroscopies are the best to detect IR-inactive bands in contrast to gas and liquid phase IR, ATR and Raman!(13). It is only possible to see the peaks corresponding to clusters with jet IR and jet Raman spectra.

MW spectral experiments provide information about the geometry(Rozas) of these kind of systems and the interaction energy from the experimental centrifugal distortion constant D_J; e.g. the interaction energy for benzene-ammonia complex is estimated as -1,4 kcal/mol from the MW spectrum (15).

NMR chemical shifts are indicative of strong shielding effects associated with the ring current of the π-stacked systems.

X-ray diffraction structures where intramolecular NH/π interactions are observed at atomic resolution, allowed us to determine precisely the parameters characterizing such unconventional interactions (25). They support the existence of both intra- and intermolecular XH/π bonding interactions (23). For example, from X-ray diffraction experiments, the structurally characterizing amino-N to benzene ring centre separation is found in the range 3,592 – 3,920 Å and the corresponding H to ring centre separation between 2,752 – 3,114 Å.

1.5 The Effects of Aromatic Hydrogen Bond on the Structure and Spectra

It is customary that every interaction has a particular effect on the structure and spectroscopic properties of the systems; aromatic H-bond displays such effects too, e.g. IR & Raman peak wavenumbers, NMR shifts, quantum yields, UV & fluorescence spectra, stability, K_a and K_b constants, anharmonicity constants, dipole moment, thermodynamic functions, packing crystal structures, etc.

IR spectral investigation has the major importance in dealing with aromatic H-bonded systems due to the easily observable character of IR peaks; especially the stretching modes play the key role due to the fact that XH/π interactions affect the vibrational dynamics of the molecules directly. Typical IR shifts are within 25 - 100 cm^{-1}. Generally; for dimers, up to 100 cm^{-1}, for trimers; up to 140 cm^{-1} and for tetramers; up to 150 cm^{-1}, etc.

It has been investigated that the stretching band of a simple acceptor molecule decreases in intensity by the existence of donor molecule via the aromatic H-bond interaction. This is concluded by an apperance of a new red-shifted peak with lower wavenumber which increases by the increasing concentration of the donor molecule, Fig. 1. Due to the XH bond weakens, when the XH bond in the donor molecule interacts with the B acceptor to form an H-bond, its stretching band in the IR spectrum shows $\Delta\tilde{\nu}$ shifts those strongly depend on the nature and the strength of the molecular acceptor! Studies showed that the shifts of the associated bands increase linearly with the pi-electron density of the substrates (27). Therefore, aromatic H-bond becomes stronger with the increasing acceptor quality and thus, the values of IR shifts becomes larger (13).

Due to its high importance on the stabilization energies, the aromatic H-bond susbtantially affects to the thermodynamic functions such as H(enthalpy), G(Gibbs free energy), S(entropy), μ(chemical potential), etc. Although sometimes being so small in magnitude, their high population -especially in biological systems- make them too much important in thermodynamic properties.

1.6 Vibrational Dynamics

1.6.1 Born-Oppenheimer (BO) Approximation

Molecular Schrödinger equation cannot be solved analytically without any approximations made. It is customary to use BO approximation to reduce the problem in an easier one by divide it into two parts; an electronic and nuclaer Schrödinger equation. One can write the full relativistic hamiltonian without any external field as (29-31,64);

$$H = -\hbar^2/2\mu_e \cdot\sum_i^N \nabla_i^2 + V(r) - \hbar^2/M \cdot \sum_{i>j}^N \nabla_i \cdot \nabla_j - \hbar^2/2(M+N.m). \sum \nabla^2_N + V_o + \sum_{A<B} Z_A.Z_B.e^2/R_{AB} - p^4/8.m^3.c^2 + \xi.S.L + \xi'.S_i.L_j + B.f(S_i.S_j) - A.B_{iç}.[f(L,S,I)+f(I,J)] + C.f(r,R) - \mu_J.B_{iç} - \mu_I.B_{iç} - \hbar^2/2\mu_n. \sum \nabla^2_N \quad \textbf{(1.5)}$$

If one neglects the relativistic corrections first, we get

$$H = H_{elec} + H_{nuc} + V_{nn} \quad \textbf{(1.6)}$$

where V_{nn} is the constant internuclear repulsion term, then

$$H.\Psi = E.\Psi \quad ; \quad \Psi = \Psi_{elec} \cdot \Psi_{nuc} \quad \textbf{(1.7)}$$

with the electronic Schrödinger equation (32-34);

$$H_e (r,R) \cdot \Psi_e (r,R) = E_e (R) \cdot \Psi_e (r,R) \quad \textbf{(1.8)}$$

and the nuclear Schrödinger equation:

$$H_{nuc} = H_{trans} + H_{relative} \quad ; \quad \Psi_{nuc} = \Psi_{trans} \,.\, \Psi_{relative} \qquad \textbf{(1.9)}$$

$$[H_{trans} + H_{relative} - E] \,.\, \Psi_{nuc}(R) = 0 \qquad \textbf{(1.10)}$$

so; the nuclear equation is further subdivided into two parts as translation and relative wave equations. But the BO approximation still continues, the *relative nuclear equation* can be still further subdivided into two parts to give a *radial equation* and an *angular equations.* Consequently, the BO approximation consists of three following subdivisions above. The resulting BO energy is a function of nuclear coordinates;

$$E_{BO} = E_e(R) + V_{nn} \qquad \textbf{(1.11)}$$

which remains a *potential energy surface* (PES). It is easy to see that the vibration and rotation motions are always coupled to each other which causes a serious problem in vibrational dynamics (35). That means one needs to go beyond to the BO approximation by further consistent approximations. HBJ approach is somewhat a good solution to meredy this problem.

Adiabatic approximation can be used to go beyond the BO approximation. The BO approximation corresponds to neglecting all of the coupling terms while the adiabatic approximation only neglects all nondiagonal coupling terms. The *nonadiabatic approximation* corresponds to the consideration all diagonal and nondiagonals as the direct calculation of the electronic-vibrational-rotational wavefunction for a molecule.

There are also additional corrections to the BO approximation as electronic-rotation coupling, mass polarization, radial motion, centrifugal correction, relativistic and quantum electrodynamical (radiative) corrections. All these terms can be calculated by the use of perturbation theory. For relativistic and quantum electrodynamical corrections, the perturbation parameter is $\alpha = 1/137$ fine structure constant; for all the others, the parameter is $1/\mu$ where μ is the reduced mass of electron.

1.6.2 Hougen-Bunker-Johns (HBJ) Approach

HBJ approach (36,37) based on using a non-rigid reference allows the transfer of the problematic motions from the vibrational part of the dynamical Hamiltonian to its rotational part. First one transforms (R,θ,φ) coordinates to the (R,ρ,σ) vibrational coordinates; then the exact kinetic energy operator is given as;

$$T^{exact} = \tfrac{1}{2}.\ \mu^{1/4}\ .\ \sum_{ij}\ J_i\ .\ \mu_{ij}\ .\ \mu^{-1/2}\ .\ J_j\ .\ \mu^{1/4} \qquad ;\quad (i,j = R,\rho,\varphi) \qquad \textbf{(1.12)}$$

where $J_R = -i\hbar.\partial/\partial R$; $J_\rho = -i\hbar.\partial/\partial\rho$, $J_\sigma = -i\hbar.\partial/\partial\sigma$ and μ_{ij} being components of the generalized 6×6 HBJ molecular inertia (I) tensor with its determinant μ:

$$I = \begin{vmatrix} I_{xx} & I_{xy} & I_{xz} & I_{xR} & I_{xr} & I_{xs} \\ I_{yx} & I_{yy} & I_{yz} & I_{yR} & I_{yr} & I_{ys} \\ I_{zx} & I_{zy} & I_{zz} & I_{zR} & I_{zr} & I_{zs} \\ I_{Rx} & I_{Ry} & I_{Rz} & I_{RR} & I_{Rr} & I_{Rs} \\ I_{rx} & I_{ry} & I_{rz} & I_{rR} & I_{rr} & I_{rs} \\ I_{sx} & I_{sy} & I_{sz} & I_{sR} & I_{sr} & I_{ss} \end{vmatrix} \qquad \textbf{(1.13)}$$

The approximate kinetic energy can be given by the diagonal μ_{ii} matrix as;

$$T^{app} = \tfrac{1}{2}.\ \sum_i\ \mu_{ii}^{0}\ .\ J_i^{2} \qquad \textbf{(1.14)}$$

with μ_{ii}^{0} is μ_{RR}^{0} , $\mu_{\rho\rho}^{0}$ and $\mu_{\sigma\sigma}^{0}$. The small magnitude of T^{exact}-T^{app} difference makes it possible to use T^{app} as the simplification of the dynamical problem. Then one uses this operator in the Schrödinger equation and solves it for the Ψ(R,ρ,σ) vibrational wavefunction. One should also use a fitted V(R,ρ,σ) potential energy.

Aromatic H-bonding supports T-shaped, cluster, floppy, stacked, etc. structure formation in pi systems. Each structure is the part of the vibrational dynamics by conformational interconventions via tunneling effects or particularly displaced transient structures; e.g. the benzene dimer is a very floppy system undergoing fast conformational interconventions between T-shaped and parallel-displaced structures due to being practically isoenergetic by a low barrier. In (θ,φ) space, the interconverting/tunneling motions depend on θ angle while φ-motion for a particular conformer shows an adiabatic separability from the θ and R-motions. R-motion is

also responsible for intermolecular stretching. If φ-motion is very adiabatically separable, it means the potential well is fairly narrow harmonic-like shaped and the PES has very flat bottoms. The adiabatic separability increases with R intermolecular distance which helps one to determine this separability of φ-motion via a few series of calculations for different R values (38).

1.7 Model Computations On Aromatic Hydrogen Bond

Supermolecular ab inito calculations are based on finding the most accurate correlation energy of the system to go beyond the HF (Hartree-Fock) orbital theory. The several computations were performed by MP2, MP4, CCSD(T), QCISD(T) and also DFT methods. HF energies have very small basis set dependence due to not involving electron correlation, this energy is mainly of orbital part and important for the electrostatic and exchange-repulsion components. Other methods including electron correlation are of course strong basis set dependent, e.g. MP2/cc-pVDZ underestimates the energy as much as 36-61 %. MP2 method generally tends to overestimate the stability of less stable isomers and it fails for the systems in which the dispersion attraction is the most important component (14,15,39). CCSD substantially underestimates the attraction compared to CCSD(T) that suggests the importance of triple excitations. CCSD(T) and QCISD(T) -which seems to the best- are the most appropriate methods when one uses very large basis sets such as aug-cc-pVTZ, etc. But one should never forget that shorter internuclear distances would be the cause of larger BSSE due to high overlap between basis functions.

It has been reported that DFT method cannot evaluate the attractive dispersion interaction in such complexes, hence DFT underestimates the interaction energy in contrast to ab initio ones. DFT has also a characteristic fuctional method dependence additional to the basis set dependence, e.g. the pyrrole dimer bond angle (important for the explanation of directionality) has been predicted as 73^0 at B3LYP and 70^0 at PW91 levels while the experimental value is 55^0 (13). That situation indicates the deficiency of density functionals in describing these complexes. Thus, DFT-D method was developed by adding some empirical dispersion corrections. DFT-SAPT is also another way in dealing with these weak complexes. Some of the calculated interaction energies were given in Table 1, in comparison to water dimer classical H-bond energy.

Table 1 : Model calculations on aromatic H-bonding in comparison with water dimer

Complexes [a]*HF/6-31G(d,p)+BSSE* [b]*CCSD(T)/basis set limit*	**Interaction Energy (kcal/mol)**
[a]Ethanol-Toluene	-1,58
[a]Ethanol-m-Xylene	-1,70
[b]Ammonia-Benzene	-2,22
[b]Water-Benzene	-3,02
[b]Methane-Benzene	-1,45
[b]Benzene-Benzene	-2,46
[b]Acetylene-Benzene	-2,83
[b]Ethylene-Benzene	-2,06
[b]Ethane-Benzene	-1,82
Water-Water	*-5,23*

Due to the diffuse electronic density of pi systems, one needs to use basis sets including diffuse functions which causes BSSE. The interaction energies are generally overestimated due to the BSSE. CP (counterpoise) approach, which works well enough to compute BSSE values, does not work well in single point computations without optimization; this is only meaningful in smaller systems. Hence, BSSE-corrected energies are somewhat in disagreement with experimental values, meaningful results are available for small basis sets where the large portion of the interaction energy cannot be evaluated however! The 50 % BSSE corrections are found more consistent instead of computing the whole BSSE for large systems (40).

1.8 Structure and Properties of Pyrazine and Triazine

Pyrazine is a heterocyclic aromatic organic compound having the D_{2h} symmetry and forming white crystals at room temperature. Its crystal structure is orthorhombic with two molecules in unit cell and the bonding parameters are R(C-N) = 1,334 Å, R(C-C) = 1,378 Å, R(C-H) = 1,05 Å, Θ(N-C-N) = 122,4^o and Θ(C-N-C) = 115,1^o (101). The

pyrazine molecule occupies a centre of symmetry in the crystal lattice. Its crystal structure was predicted as formed with T-shaped structures (101,103).

The studies on the acidities of liquid pyrazine derivaties have shown that the C-H…N interaction is stronger than the C-H…π one in terms of C-H donor and N and π acceptors. For the C-H…N interactions, the H…N distance was found to be decreased with increasing C-H acidity (102).

The structures of pyrazine dimer were studied theoretically (14) in comparison to experimental data and the doubly-bridged dimer structure was found as the most stable conformation by two CH…N contacts, Fig.3.

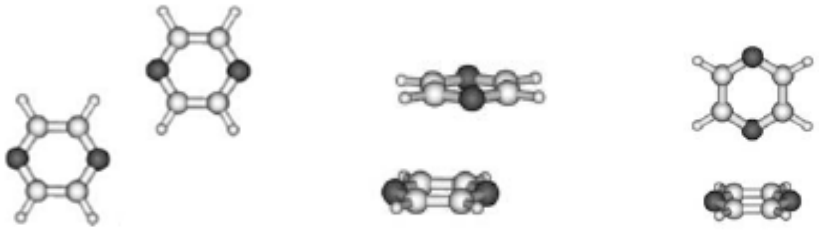

Figure 3 : Doubly-bridged, cross-displaced and T-shaped structures of pyrazine dimer

The cross-displaced stacked dimer structure and the T-shaped one were also found as the second and third most stable conformations respectively. But, it was reported that the most stable doubly-bridged dimer did not directly reflect the structural motif of the pyrazine crystal (14).

Pyrazine has zero dipole moment, but a non-zero quadrupole moment. Thus, a quadrupole-quadrupole interaction is expected to play a key role in the geometry of the dimer. Although dispersion interaction is maximum for the sandwich configuration, it was found that the substantial electrostatic repulsion and exchange repulsion make it unstable (103).

There are three types of triazine found purely in nature as 1,2,3-; 1,2,4- and 1,3,5-triazine which are three different chemicals, Fig.4. Thus, they perform different chemical properties and reactions. Their synthesis pathways are also completely different. The computations predict the 1,3,5-triazine as the most stable one which is also called as *s-triazine*. 1,3,5-triazine has two different crystal structures with respect to temperature; as rhombohedral and monoclinic. This shows that 1,3,5-triazine crystal is not a mixture of these two different structures, it displays a definite

crystal structure; e.g. rhombohedral at room temperature. The XRD studies have shown that 1,3,5-triazine has doubly-bridged structure in the crystal phase (104,105)

Figure 4 : Structures of 1,2,3-; 1,2,4- and 1,3,5-triazines

Unlike the benzene molecule which has a negative electrostatic potential inside the carbon ring, triazines have positive electrostatic potential inside the ring and all the nitrogen including regions outside the ring have negative electrostatic potential, this is the reason for the stacked triazine dimer structures in contrast to T-shaped like benzene dimers.

The dimeric interactions in triazines have been found stronger than the benzene ones due to the higher polarizabilities of triazines.

In nitrogen containing cyclic systems, it was concluded that the pi electron density decreases and the electrostatic potential increases inside the ring with respect to increasing number of nitrogen atoms. That supplies a substantial reduction in pi electronic repulsion between donor and acceptor species and a stronger dimer interaction remains; e.g. Tz(1,3,5) – Bz [-3,75 kcal/mol], Tz (1,3,5) – Tz [-3,03 kcal/mol] and Bz – Bz [-2,78 kcal/mol]. The symmetry of the ring structure also causes a decrease in the number of possible dimeric configurations.

1.9 Theory of Intermolecular Forces

There is now general aggreement that the significant forces betwen atoms and molecules have an electric origin. It is true that other sources exist, such as magnetic and gravitational interactions, but these can normally be neglected. Thus, one needs to deal with an electrostatic Hamiltonian for a set of interacted systems.

Choosing the zeroth-order Hamiltonian to be the sum of the electrostatic Hamiltonians for the two separated systems,

$H_0 = H_a(i) + H_b(j)$ **(1.15)**

the complete electrostatic H for AB system is,

$H_e = H_0 + V_e$ **(1.16)**

and the electrostatic approximation to the perturbational potential is given by

$$V_e = H_e - H_0 = -\sum_j \frac{Z_a}{r_{aj}} - \sum_i \frac{Z_b}{r_{bi}} + \sum_{i>j} \frac{1}{r_{ij}} + \frac{Z_a Z_b}{R} \quad \textbf{(1.17)}$$

Whereas variational techniques are especially suited for the calculation of short and intermediate range intermolecular forces; perturbational techniques are suited for the calculation of long range forces. It is frequently desirable to express the interaction (or perturbation) potential V_e in terms of a multipole expansion due to the fact that the separation is large at long range, compared to the dimensions of the molecules, the interaction energy is determined by the permanent electric moments. For those electronic configurations where the separation is sufficiently large that $R > (r_{ai} + r_{bj})$ for all i and j, the r_{ai}^{-1} and r_{bj}^{-1} can be expanded in Neumann series and the r_{ij}^{-1} can be expanded in a bipolar series to give the interaction potential in the form

$$Ve = \sum_{n=1}^{\infty} \frac{V_n}{R^n} \quad \textbf{(1.18)}$$

Where V_n coefficients represent the instantaneous interaction of the various multipoles; e.g. V_1 is the charge-charge interaction, V_2 is the charge-dipole interaction, V_3 is the sum of the dipole-dipole and charge-quadrupole interactions, etc. Both of cartesian and spherical tensors can be used in multipole expansion. The spherical formulation requires the use of Clebsh-Gordon and Racah coefficients and also 3-j, 6-j and 9-j symbols.

There are two approaches to the calculation of the interaction energy: *polarization expansion* and *multipole expansion* [18,19,88]. The latter one is more convenient to get the explicit forms of different interactions. The multipole expansion of the interaction potential, which is an asymptotic expansion, is very convenient for a conceptual understanding of long range intermolecular forces. Combined with the perturbation theory outlined above, it leads to a formal series expansion of both E_{AB} and ψ_0 in powers of R^{-1}:

$$E_{AB} = \sum_n \frac{C_n}{R^n} \quad \textbf{(1.19)}$$

$$\Psi_0 = \Phi_0 + \sum_{n=1}^{\infty} \Phi_n R^{-n} \quad \textbf{(1.20)}$$

where Φ_0 is the wavefunction for the separated systems. C_n coefficients can be calculated by variational techniques.

In the sense of multipole expansion, the interacitons of permanent electric moments comprise the "*electronic energy*". The permanent moments produce a field that distorts the electronic structures of neighbouring molecules leading to an additional interaction, "*induction energy*". Since the distortion of molecules in their ground electronic states always lower the total energy, the induction energy is associated with an attractive intermolecular force. "*Dispersion energy*" is related to the polarizabilities describing the distortion of the free molecules by electrical fields.

The Hamiltonian of a molecule in an electric field is

$$H = H^{(0)} - \mu_\alpha \,.\, F_\alpha - \frac{1}{3} \,.\, \theta_{\alpha\beta} \,.\, F_{\alpha\beta} - \ldots\ldots\ldots \quad \textbf{(1.21)}$$

where $H^{(0)}$ is that for the free molecule and μ_α and $\theta_{\alpha\beta}$ are dipole and quadrupole moment operators respectively. When there are two sytems interacting to each other and far apart, electron exchange can be neglected and the H_{int} treated as a perturbation Hamiltonian.

$$H' = \sum_{i_1,i_2} e_{i_1} e_{i_2} \,.\, R_{i_1 i_2}^{-1} = q_2.\Phi_2 - \mu_{2\alpha} \,.\, F_{2\alpha} - \frac{1}{3} \,.\, \theta_{2\alpha\beta} \,.\, F_{2\alpha\beta} - \ldots\ldots$$

$$= q_1.\Phi_1 - \mu_{1\alpha} \,.\, F_{1\alpha} - \frac{1}{3} \,.\, \theta_{1\alpha\beta} \,.\, F_{1\alpha\beta} - \ldots\ldots \quad \textbf{(1.22)}$$

for $E_1^{(0)} + E_2^{(0)}$ and $\psi_1^{(0)}.\psi_2^{(0)}$. The H_{int} can be written as a multipole expansion; then the energy of the pair may be obtained from the perturbation theory,

$$E_{n1,n2} = E_{n1}^{(0)} + E_{n2}^{(0)} + \left\langle \Psi_{n1}^{(0)} \Psi_{n2}^{(0)} \middle| H' \middle| \Psi_{n1}^{(0)} \Psi_{n2}^{(0)} \right\rangle - \sum \frac{\left[\left\langle \Psi_{n1}^{(0)} \Psi_{n2}^{(0)} \middle| H' \middle| \Psi_{j1}^{(0)} \Psi_{j2}^{(0)} \right\rangle \right]^2}{\left(E_{j1}^{(0)} - E_{n1}^{(0)} \right) + \left(E_{j2}^{(0)} - E_{n2}^{(0)} \right)} + \ldots \quad \textbf{(1.23)}$$

The first-order energy is the electronic energy:

$$u_{elec}^{(n1,n2)} = \left\langle \Psi_{n1}^{(0)} \Psi_{n2}^{(0)} \middle| H' \middle| \Psi_{n1}^{(0)} \Psi_{n2}^{(0)} \right\rangle = T_2.q_1.q_2 + T_{2\alpha} \,.\, (q_1 \mu_{2\alpha}^{(n2)} - q_2 \mu_{1\alpha}^{(n1)}) +$$

$$T_{2\alpha\beta} \,.\, (\frac{1}{3} \,.\, q_1.\theta_{2\alpha\beta}^{(n2)} + \frac{1}{3} \,.\, q_2 \,.\, \theta_{1\alpha\beta}^{(n1)} - \mu_{1\alpha}^{(n1)} \mu_{2\beta}^{(n2)}) + \ldots. \quad \textbf{(1.24)}$$

The second-order energy includes both the induction and dispersion energy:

$$u_{ind}^{(n1,n2)} = -\sum \frac{[\langle \Psi_{n1}^{(0)} \Psi_{n2}^{(0)} | H' | \Psi_{j1}^{(0)} \Psi_{n2}^{(0)} \rangle]^2}{\left(E_{j1}^{(0)} - E_{n1}^{(0)}\right)} - \sum \frac{[\langle \Psi_{n1}^{(0)} \Psi_{n2}^{(0)} | H' | \Psi_{n1}^{(0)} \Psi_{j2}^{(0)} \rangle]^2}{\left(E_{j2}^{(0)} - E_{n2}^{(0)}\right)} \quad \textbf{(1.25)}$$

$$u_{disp}^{(n1,n2)} = -\sum \frac{[\langle \Psi_{n1}^{(0)} \Psi_{n2}^{(0)} | H' | \Psi_{j1}^{(0)} \Psi_{j2}^{(0)} \rangle]^2}{\left(E_{j1}^{(0)} - E_{n1}^{(0)}\right) + \left(E_{j2}^{(0)} - E_{n2}^{(0)}\right)} \quad \textbf{(1.26)}$$

$$= -\sum_{\substack{j1 \neq n1 \\ j2 \neq n2}} T_{2\alpha\beta} T_{2\gamma\delta} \frac{\langle \Psi_{n1}^{(0)} \Psi_{n2}^{(0)} | \mu_{1\alpha} \mu_{2\beta} | \Psi_{j1}^{(0)} \Psi_{j2}^{(0)} \rangle \langle \Psi_{j1}^{(0)} \Psi_{j2}^{(0)} | \mu_{1\gamma} \mu_{\delta 2} | \Psi_{n1}^{(0)} \Psi_{n2}^{(0)} \rangle}{\left(E_{j1}^{(0)} - E_{n1}^{(0)}\right) + \left(E_{j2}^{(0)} - E_{n2}^{(0)}\right)} + ..]$$

Therefore, the dispersion energy for the molecules in their ground states varies as R^{-6} for large R with additional contributions in R^{-7}, R^{-8}, etc. due to the definition of T_2 tensor.

In the polarization expansion formalism, energy is called as "*polarization energy*" in each order. Thus, the first-order polarization energy is electrostatic energy, the second-order polarization energy is the sum of induction and dispersion energies, etc. In the long range, the perturbation energy in each order can be purely called as polarization energy; but in the short range, the perturbation energy is the sum of polarization and exchange energies in each order. This is the starting point of "*Symmetry Adapted Perturbation Theory* (SAPT)" formalism.

1.10 Symmetry Adapted Perturbation Theory

Although the interaction energy is very small, the change in the wavefunction due to the perturbation potential is not small. The unperturbed and perturbed wavefunctions are located in different parts of the Hilbert space and they are not close to each other even at large separations. A finite polarization treatment does not recover the electron exchange which is important in short and intermediate ranges. For that reason, the "*Rayleigh-Schrödinger Perturbation Theory* (RSPT)" breaks down and one needs to use alternative perturbation formulations.

Due to the fact that important contributions to the wavefunction can be recovered by an appropriate symmetry projection, an alternative formulation can be treated by using symmetry considerations which is called "*Symmetry Adapted Perturbation Theory* (SAPT)" [89,90]. Numerous SAPT formulations have been proposed.

At sufficiently large R, the truncated polarization series can be given as –in the asymptotic relationship-

$$V_{AB} = \sum_{k=1}^{n} E_{pol}^{(k)} + O(R^{-\kappa(n+1)}) \quad \textbf{(1.27)}$$

where κ = 2 if at least one of the interacting molecules has a net charge and κ = 3 if both molecules are neutral. After an appropriate symmetry projection, the polarization expansion of the wavefunction gives the correct asymptotic expansion wavefunction as;

$$\Psi_{AB} = \hat{A} \,.\, \Phi_0 + \sum_{k=1}^{n} \hat{A}\, \Phi_{pol}^{(k)} + O(R^{-\kappa(n+1)}) \quad \textbf{(1.28)}$$

where $\hat{A}$ is the (N_A+N_B)-electron antisymmetrizer as the product of each antisymmetrizers.

The simplest approach to the symmetry adaptation is based on these equations which show that by symmetrizing a finite sum of the polarization series, one obtains a very good asymptotically exact approximation to the wavefunction. Then, n-th order $\Phi_{pol}(n)$ function is given by

$$\Phi_{pol}(n) = \Phi_0 + \Phi_{pol}^{(1)} + \Phi_{pol}^{(2)} + \ldots\ldots\ldots + \Phi_{pol}^{(n)} \quad \textbf{(1.29)}$$

and $\hat{A}.\Phi_{pol}(n)$ involves all resonance structures resulting from electron exchange. Thus, such kind of wavefunction can be safely used in both short and intermediate ranges. Then, the energy is;

$$E(n) = \frac{\langle \Phi_0 | V | \hat{A}\Phi_{pol}(n) \rangle}{\langle \Phi_0 | \hat{A}\Phi_{pol}(n) \rangle} \quad \textbf{(1.30)}$$

To obtain the individual energy correction terms, a parameterization is required:

$V \rightarrow \xi \,.\, V$

$\Phi_{pol}^{(k)} \rightarrow \xi^{k} \,.\, \Phi_{pol}^{(k)}$

Now, the energy expression can be expanded as a power series in ξ;

$$E(n) = \xi \,.\, E^{(1)} + \xi^{2} \,.\, E^{(2)} + \ldots\ldots\ldots + \xi^{n} \,.\, E^{(n)} \quad \textbf{(1.31)}$$

where the first-order energy is

$$E^{(1)} = \frac{\langle \Phi_0 | V | \hat{A}\Phi_o \rangle}{\langle \Phi_0 | \hat{A}\Phi_o \rangle} \quad \textbf{(1.32)}$$

and the second-order energy is

$$E^{(2)} = \frac{\langle \Phi_0 | V - E^{(1)} | \hat{A}\Phi_{pol}^{(1)} \rangle}{\langle \Phi_0 | \hat{A}\Phi_o \rangle} \quad \textbf{(1.33)}$$

When $\hat{A}$ is replaced by the identity operator, $E^{(n)}$ corrections reduces to the polarization energy $E_{pol}^{(n)}$ and an exchange part remains:

$$E^{(n)} = E_{pol}^{(n)} + E_{exch}^{(n)} \quad \textbf{(1.34)}$$

If one writes the Â operator in terms of permutaion operator P; first- and second-order exchange energies occur as;

$$E_{exch}^{(1)} = \frac{\left\langle \Phi_0 \middle| V(P - \langle P \rangle) \middle| \Phi_{pol}^{(1)} \right\rangle}{1 + \langle P \rangle} \quad \textbf{(1.35)}$$

$$E_{exch}^{(2)} = \frac{\left\langle \Phi_0 \middle| (V - E^{(1)})(P - \langle P \rangle) \middle| \Phi_{pol}^{(1)} \right\rangle}{1 + \langle P \rangle} \quad \textbf{(1.36)}$$

Thus, the second-order exchange energy is a result of the antisymmetrization of the first-order polarization function and sometimes called as "exchange-polarization energy". Since the first-order polarization function is the sum of the induction and dispersion components;

$$\Phi_{pol}^{(1)} = \Phi_{ind}^{(1)} + \Phi_{disp}^{(1)} \quad \textbf{(1.37)}$$

where $\Phi_{ind}^{(1)}$ and $\Phi_{disp}^{(1)}$ comes from the simple RSPT by a polarization expansion; then the exchange energy becomes;

$$E_{exch}^{(2)} = E_{exch\text{-}ind}^{(2)} + E_{exch\text{-}disp}^{(2)} \quad \textbf{(1.38)}$$

Consequently, the exchange-induction and exchange-dispersion energies appear since the induction and dispersion contributions to the wavefunction are symmetrized in the second-order energy expression. In the short range, the exchange-induction energy quenches an important part of the induction contribution and cannot be neglected. The exchange-dispersion energy is less important due to it quenches almost 10 % of the dispersion energy.

Up to second-order, one can write

$$V_{AB} = V_{AB}^{HF} + V_{AB}^{corr} \quad \textbf{(1.39)}$$

then easily separate the HF and correlation contributions to the interaction energy explicitly:

$$V_{AB}^{HF} = E_{el}^{(1)} + E_{exch}^{(1)} + E_{ind}^{(2)} + E_{exch\text{-}ind}^{(2)} \quad \textbf{(1.40)}$$

$$V_{AB}^{corr} = E_{disp}^{(2)} + \epsilon_{el}^{corr} + \epsilon_{ind}^{corr} + \epsilon_{exch}^{corr} \quad \textbf{(1.41)}$$

Finally, all the higher order induction, induction-dispersion and exchange-induction corrections are collected by a δE_{HF} term, then one gets;

$$E_{int} = E_{el}^{(1)} + E_{exch}^{(1)} + E_{ind}^{(2)} + E_{disp}^{(2)} + E_{exch\text{-}ind}^{(2)} + E_{exch\text{-}disp}(2) + \delta E_{HF} \quad \textbf{(1.42)}$$

Very often the pairwise additivity approximation is insufficient and three and more body contributions are necessary. To study systems containing more than two

molecules, the complete intermolecular potential $V_{ABC...}$ can be written in the form of the many body expansion

$$V_{ABC...} = \sum_{X<Y} V_{XY}[2] + \sum_{X<Y<Z} V_{XYZ}[3] + \ldots\ldots \quad \textbf{(1.43)}$$

where

$V_{XY}[2] = V_{XY}$;

$V_{XYZ}[3] = V_{XYZ} - V_{XY} - V_{YZ} - V_{XZ}$; etc.

Of course, the pairwise additions (first term in the expansion) indeed are responsible for the major contributions and is sufficient for many purposes. The higher-body interactions (nonadditive approximation) can be treated by using the theory of intermolecular forces in liquids in a general way [88].

Recently, nonadditive SAPT corrections for trimers and tetramers have been developed although being not so satisfactory; e.g. $E_{disp}^{(3)}[3]$, $E_{ind}^{(2)}[3]$, $E_{exch}^{(1)}[3]$, $E_{ind}^{(3)}[3]$, $E_{exch-ind}^{(2)}[3]$, $E_{exch-disp}^{(2)}[3]$, $E_{ind-disp}^{(3)}[3]$ and $E_{disp}^{(4)}[3]$.

In essence, SAPT expresses the interaction energy with an additional exchange interaction;

$$V_{AB} = \sum_{n=1}^{\infty} E_{pol}^{(n)} + \sum_{n=1}^{\infty} E_{exch}^{(n)} \quad \textbf{(1.44)}$$

While simple RSPT treats the same potential as;

$$V_{AB} = \sum_{n=1}^{\infty} E_{pol}^{(n)} \quad \textbf{(1.45)}$$

SAPT results converge to the CP-corrected ab initio ones. Additionally, it converges faster when standart correlation energy-optimized basis sets are used. The major speedup of convergence appears in the dispersion energies.

2. METHODS

2.1 Many Electron Problem

The Schrödinger equation of the many electron systems cannot be solved analytically due to the existence of the interelectronic repulsion term in the Hamiltonian. Hartree-Fock (HF) theory (41,42,43) is the excellent solution of the orbital part of the problem which was proved then by the X ray diffraction maps fit perfectly with the electronic distribution maps (44). The remaining part is the correlation part of the exact wavefunction. HF theory uses the full Hamiltonian in the variational calculation of the energy; but this is only an energy of the full Hamiltonian corresponding to the HF determinant (Φ_o) as our trial orbital wavefunction:

$E_{HF} = < \Phi_o \mid H \mid \Phi_o >$ **(2.1)**

In 1959, P. O. Löwdin defined the nonrelativistic correlation energy as;

E_{corr} (nonrelativistic) = E (nonrelativistic) – E_{HF} **(2.2)**

where E_{HF} is the HF limit energy (45). A more general and comprehensive definition was made in the relativistic sense (46):

$E_{corr} = E - E_{HF} - E_{rel}$ **(2.3)**

where E_{rel} involves all relativistic corrections such as; relativistic kinetic energy of the electrons, spin-orbit interaction, hyperfine interaction, etc. But, it still needs some quntum electrodynamical corrections (maybe a E_{QED} term can be substracted as well).

Electron correlation is not only a concept in the basis of energy; in contrast, it is a fundamental phenomenon and has a deep effect on many quantities additional to the energy. There are some quantities they should never be computed without electron correlation; such as total energy, dipole moment, electron affinity, polarizability and hyperpolarizabilities, binding energy (BE) , excited states and oscillator strengths. For example, a dipole moment calculation absolutely requires the single electron

correlation; thus if a correlation method does not involve any single excitations such as CID, etc., is not suitable for dipole moment (47).

In 1950s, the insufficient computations made some theoreticians believe that the odd numbered electron correlations (singles, triples, etc.) are more important than the even numbered electron correlations (doubles, quadruples, etc.) But in 1960s, better CI calculations showed a proof in the opposite direction; e.g. for Be atom (48), the quadruples had a larger contribution to the energy and wavefunction than the triples! Moreover, single excitations are not necessary for the energy calculations; they are only important for dipole moment and excited states. Therefore, an electron correlation method should at least contain the quadruples.

In the many electron problem, another question is the competition between the basis set extension and the number of configurations. Energy approaches to the full CI result by the increasing number of configurations in contrast to the basis set extension in which the energy approaches to the HF limit. So, what about the exact energy? The exact nonrelativistic energy is available by the simultaneous increasing of both. But in practice, both situations are not possible. Does it means that we can never have a good many electron theory?

A good electron correlation theory should be independent of both basis set extension and number of configurations; e.g. an IEPA calculation for Be with a sufficient basis set gives the 99 % of the exact nonrelativistic correlation energy although considering only the 1s and 2s states and their mixed configurations (49). This example is also the reason for another case because one may also think that 100 % of the correlation energy can be obtained by a basis set extension. This is not meaningful; otherwise there would always be a possible complete basis set special for every atom or molecule and also we would never understand the completeness of these sets without any experimantal data!

Consequently; a many electron theory should be;

- general (applicable) for all systems
- a finite series expansion of the n-tuply excitations
- basis set independent (should not require basis set completeness)
- a rigorous analysis of the fluctuation potential responsible for the correlation
- invariant under unitary transformations
- variational
- size consistent

2.2 Many Electron Theory (MET)

In the exact Many Electron Theory (MET) , the exact wavefunction of a many electron system is;

$$\psi = \Phi_o + \chi \qquad \textbf{(2.4)}$$

with the strictly defined normalization and orthogonalization conditions as

$$\langle \Phi_o \mid \chi \rangle = 0 \qquad ; \qquad \langle \psi \mid \psi \rangle = 1 + \langle \chi \mid \chi \rangle \qquad \textbf{(2.5)}$$

where Φ_0 is the HF determinant and χ is the correlation function; then the exact energy of a many electron system is given as in the expression below:

$$E = \frac{\langle \chi | H\psi \rangle}{\langle \chi | \chi \rangle} = E_{HF} + \frac{2\langle \phi_0 | (H - E_{HF})\chi \rangle + \langle \chi | (H - E_{HF})\chi \rangle}{1 + 2\langle \phi_0 | \chi \rangle + \langle \chi | \chi \rangle} \qquad \textbf{(2.6)}$$

According to the MET (46,50,51) and the observations made on the available computational data, the even numbered electron correlations are so much important than the odd numbered electron correlations in terms of their contributions to the correlation energy. In this sense, the exact corrrelation function may be first given as the sum of all possible n-electron clusters and then, N electron problem is easily reduced to N(N-1)/2 two electron problems by representing each n-electron cluster correlation function with the binary correlations which are taken place in a spatial region simultaneously; because it is difficult to collide more than two electrons at the same time as in the imperfect gas theory (52);

$$\chi \approx \chi_s' = A \,.\, \{ (123.....N) [(2!)^{-1/2} \sum_{i>j}^{N} \frac{\hat{u}_{ij}}{(ij)} + (2!)^{-1} \sum_{i>j}^{N} \sum_{k>l}^{N} \frac{\hat{u}_{ij}\hat{u}_{kl}}{(ijkl)} + (2!)^{-3/2} \sum_{i>j}^{N} \sum_{k>l}^{N} \sum_{m>n}^{N} \frac{\hat{u}_{ij}\hat{u}_{kl}\hat{u}_{mn}}{(ijklmn)} + ...]\} \qquad \textbf{(2.7)}$$

where $\hat{u}_{ij}$ functions are two electron correlations and the complete χ is antisymmetrized by *A*. For example, the collision of four electrons into two independent but simultaneously two binary collisions is more possible than the four electron colision and hence, one may write down the n-electron correlation terms as the products of two electron $\hat{u}_{ij}$ correlations. That is the perfect explanation of the quadruples in the CI expansion, because the linked four electron correlations only calculates the 10 % of the quadruple correlation energy where the remainig 90 % comes from the $\hat{u}_{ij}\hat{u}_{kl}$ unlinked products. The main source of the exact character of

the MET is the deeply analysis of the fluctuation potential in the Hamiltonian hidden in the simple g_{ij} term.

CC (Coupled cluster) and BD (Brueckner doubles) perturbation theories are the simpler approximations to MET and were derived directly from it by using perturbation approach, unlike MET is completely variational. CCSD(T) is still the best variant of MET in today's computational chemistry.

2.3 Ab Initio Methods

There are two main approaches to the solution of Schrödinger equation; ab initio methods and semiempirical methods. In an ab initio calculation, one starts from the direct nonempiric solution of the Schrödinger equation except from somewhat meaningful integral approximations in contrast to a semiempirical calculation in which some parameters are used to evaluate integrals rapidly and decrease the cost of the computation. The accuracy of an ab initio calculation is determined primarily by the model chosen for the wavefunction. For large systems, ab initio methods are computationaly expensive and semiempiricals have been developed to treat a wider variety of chemical species.

2.3.1 Configuration-Interaction (CI) Theory

The basic idea of CI is to diagonalize the N-electron Hamiltonian in a basis of N-electron functions (Slater determinants) . In other words, we present the exact wave function as a linear combination of N-electron trial functions are all Slater determinants corresponding to the particular configurations; for a given arbitrary set of 2K one-electron spin orbitals, we can construct $\binom{2K}{N}$ different Slater determinants (one of them is ground state "HF determinant") . If we work with a finite set of spin orbitals (2K), then the $\binom{2K}{N}$ determinants formed from these spin orbitals do not form a complete N-electron basis. Nevertheless, diagonalizing the finite H matrix formed from this set of determinants leads to solutions that are exact within the one-electron subspace spanned by 2K spin orbitals or, equivalently, within the N-electron subspace spanned by the $\binom{2K}{N}$ determinants. This procedure is called "full CI". (In contrast to the common belief, full CI does not correspond a complete basis set! It uses all possible –full number of- determinants (configurations) in a finite basis set)

Thus, the exact nonrelativistic energy of a many electron system is obtained by "complete basis set ⊕ full CI". Even for relatively small systems and minimal basis sets, the number of determinants that must be included in a full CI calculation is truly enormous. Hence, in practice, one must truncate the full CI expansion and use only a small fraction of the $\binom{2K}{N}$ possible determinants; such as CIS, CISD, CISD(T), QCISD(T), etc., which are obtained by truncating the N-electron trial function at some excitation level:

$$\Psi = c_o \,.\, \Phi_o + \sum_{ar} c_a^r \,.\, \Phi_a^r + \sum_{abrs} c_{ab}^{rs} \,.\, \Phi_{ab}^{rs} + \ldots\ldots\ldots\ldots \quad \textbf{(2.8)}$$

A factor $(1/n!)^2$ is included in front of the summation including n-tuply excited determinants to insure that a given excitation is really counted but once:

$$\Psi = c_o \,.\, \Phi_o + (1/1!)^1 \sum_{ar} c_a^r \,.\, \Phi_a^r + (½!)^2 \sum_{abrs} c_{ab}^{rs} \,.\, \Phi_{ab}^{rs} + \ldots\ldots\ldots \quad \textbf{(2.9)}$$

i.e., $c_{ab}^{rs} \,.\, \Phi_{ab}^{rs} = c_{ba}^{rs} \,.\, \Phi_{ba}^{rs} = c_{ab}^{sr} \,.\, \Phi_{ab}^{sr} = c_{ba}^{sr} \,.\, \Phi_{ba}^{sr}$

For a basis set that is not complete, one finds the "basis set correlation energy" and full CI is the best that one can do with such a basis! As the one-electron basis set approaches to completeness, the basis set correlation energy approaches the "exact correlation energy"; that is of "complete basis set ⊕ full CI" as had been said before. For example, a double zeta basis including "p" polarization functions on hydrogen for BeH_2, full-CI gives only about 75 % of the exact correlation energy (53) although 28639 spin and symmetry adapted configurations! (Since it has 6 electrons, full CI includes all excitations up to hextuples)

There are also some kinds of truncated CI methods (except CIS, CISD, etc.) which were developed to meredy some of the problematics of CI as; MCSCF (Multiconfigurational self consistent field theory), GVB (Generalized valence bond theory) and CASSCF (Complete active space self consistent field theory) (54,55,56).

2.3.2 Coupled Cluster (CC) Theory

If one starts with a complete form of full eq.(2.7) including full S,T,Q,5, etc. correlations coming from MET and then uses the fundamental approach of it on double correlations, the following cluster expression is found:

$$\Psi_{CC} = \Phi_o + T_1.\Phi_o + (\frac{1}{2!}.T_1^{\,2} + T_2).\Phi_o + (\frac{1}{3!}.T_1^{\,3} + T_1.T_2 + T_3).\Phi_o + \ldots\ldots \quad \textbf{(2.10)}$$

where T_n is the n-electron cluster operator. In CI language, this is analogous to

$$\Psi_{CI} = \Phi_o + S + D + T + Q + 5 + 6 + 7 + 8 + ... \quad \textbf{(2.11)}$$

(In general, the CI expansion up to octuples is enough to be considered as full CI). Then one solves the eigenvalue equation for CC wavefunction:

$$(H - E_0) \, . \, \Psi_{CC} = E_{corr} \, . \, \Psi_{CC} \quad \textbf{(2.12)}$$

This approximation is known as "Coupled Pair Many Electron Theory (CPMET)" which is also called "Coupled Cluster Theory (CC)", by J. Cizek in 1966 (57,58) who derived this theory directly from MET by the perturbation approach. In practice, one may also start directly with eq.(2.7), using the fundamental approach of MET on double correlations; then several truncations become possible, e.g. for any molecule, CCSD means that the all n-electron correlations are represented by using singles(T_1) and doubles(T_2) as;

$$\Psi_{CCSD} = \Phi_o + T_1.\Phi_o + (\frac{1}{2!}.T_1^{\,2} + T_2).\Phi_o + (\frac{1}{3!}.T_1^{\,3} + T_1.T_2).\Phi_o + ... \quad \textbf{(2.13)}$$

If CISDTQ5678 is recognized as full CI in both short and longe ranges, CCSDTQ567 is the best approximation to MET and it seems like the exact solution of the Schrödinger equation. In practice, 7 and 8 electron correlations are also negligible in longe range which corresponds to CISDTQ56 as full CI, then CCSDTQ5 becomes the highest level computational method within a perfect chemical accuracy. In the basis set limit, CCSDTQ5 gives the 99,99 % of the exact nonrelativistic correlation energy (63,65). Unlike CI, the correlation energy within the CC approximation cannot be obtained by simple matrix diagonalization. CC is a perturbation theory in essence, it calculates the correlation energy of the exact correlation function of MET by perturbation theory; hence it can be considered as a perturbative variant of MET. It incorporates coupling between different pairs just as the matrix elements of the form $<\Psi_{ab}^{\,rs}, H\Psi_{cd}^{\,tu}>$. Furtherly, according to the Maclaurin expansion above, e.g. coefficients for hextuples is given as the cube of the coefficients of the doubles and so on; this is an approximation too. In CC, we made the approximation, e.g. for quadruples;

$$c_{abcd}^{\,rstu} \approx c_{ab}^{\,rs} \, . \, c_{cd}^{\,tu} - < c_{ab}^{\,rs} * c_{cd}^{\,tu} > \quad \textbf{(2.14)}$$

where $< c_{ab}^{\,rs} * c_{cd}^{\,tu} >$ represents the sum of all possible products of such double excitations. Due to CC have a complicated structure, it can be approximated by two main possible ways; "linear CC (L-CCA)" and "Coupled Electron Pair Approximation (CEPA)". The simplest approximation is to set the sum above equal to zero in CC equation which is called L-CCA because of eliminating the nonlinear

terms. Instead of ignoring all the terms involving this sum, we retain those where c=a and d=b, thus we have a better approximation than L-CCA which is called as CEPA. The major advantage of CEPA over CCA is that it is much simpler computationally; but the L-CCA should work better than CEPA when applied to a variety of molecules (47).

Recently, CCSD(T) is available in some program codes as the "gold standart" of modern ab initio computations. CCSD(T) means a CCSD(MP4-SDQ) calculation with an additional MP4-T and MP5-T contributions.

The CC2 model is an approximated second-order CCSD method for response calculations on molecules which are out of reach for CCSD and higher correlated methods [98]. It is one of the simplest correlated ab initio methods for excited states and yields energies for singly-excited states which are correct through second-order, as the well-known MP2 does for the ground states. It is thus well-suited for the study of excited states of large closed shell molecules. In difference to the perturbative doubles corrections CIS(D) to widely used CIS method and similar perturbative approaches to excited states which use nondegenerate perturbation theory, CC2 is not limited to energetically isolated states. A feature, which is important in the search of excited state equilibrium structures. Recently, it is widely used with RI integral approximation as RICC2 model (100).

2.3.3 Moeller-Plesset Perturbation Theory (MPPT)

Simple perturbation theory, also known as Rayleigh-Schrödinger perturbation theory (RSPT) can be applied to the many particle problem which is the most general problem in 'Many Body Theory'. In treating infinite systems, of course one needs a theory that is size consistent, such as nuclear matter, the RS perturbation expansion is a suitable method which is called "Many Body Perturbation Theory (MBPT)" developed by K. Brueckner and J. Goldstone as a diagrammatic perturbation theory in 1950s (59). Likewise, RSPT can be applied to N-electron systems as the most important one of all many body problems. Since we are interested in obtaining a perturbation expansion for the correlation energy, we choose the HF hamiltonian as our zeroth-order hamiltonian. RSPT with this choice of Hamiltonian was applied to N-electron systems in Quantum Chemistry by C. Moeller and M.S. Plesset (60) and hence it is called as MPPT (shortly MPN for Nth order) as the special variant of most

general MBPT. If we have chosen H_0 wisely, then V is small and the perturbation expansion converges quickly (that corresponds to a big increase between Nth and the following (N+1)th order) .

MBPT is size consistent in each order and one finds in treating large systems that they contain terms proportional to the square of the number of particles. Brueckner was able to show that these ill-behaved terms actually cancel and thus MBPT was size consistent in each order. He could not prove the fact that this was the case for all orders. In order to prove such a theorem, J. Goldstone used R. Feynman's 'Diagrammatic Perturbation Theory' in Quantum Electrodynamics and devised a pictorial representation of the expansion. He found that in each order the ill-behaved terms were represented by 'unlinked diagrams' which always cancel in every order. This is the famous "linked cluster theorem" which says that the perturbation expansion of the energy of a many body system can be represented by linked diagrams (This linked-unlinked terms are different from the similar terms in MET!)

MPPT is commonly used in MP2 up to MP7 and recently in 8th order, MP8. Every order has its own properties and problems. It is interesting to note that the fraction of the basis set correlation energy obtained at second-order increases significantly with the size of the basis. Thus, it is dangerous to draw conclusions about the utility of perturbation theory from small basis set calculations. It can be seen that the perturbation expansion converges quickly for the larger basis sets and that the correlation energy obtained through third order is in good aggreement with the exact value for the basis.

One also needs to add all possible n-tuply excitations to MP-N expansion in a given order to get the "Full MP-N" result; hence we have MP4SDTQ, MP5SDTQ, MP6SDTQ56, etc. (66,67)

The MP2 energy is the sum of the correlation energies of electrons with parallel and antiparallel spin as;

$$E_{corr}\,(MP2) = E_{corr}\,(\downarrow\downarrow) + E_{corr}\,(\uparrow\downarrow) \qquad \textbf{(2.15)}$$

But, as we know that the HF theory involves a big amount of the correlation of electrons with parallel spin as spin correlations, thus one should scale the energy to the correlation of antiparallel electrons; because they cannot make equal contribution to total correlation energy:

$$E_{corr}\,(MP2) = c_1 \,.\, E_{corr}\,(\downarrow\downarrow) + c_2 \,.\, E_{corr}\,(\uparrow\downarrow) \qquad \textbf{(2.16)}$$

Here, Grimme's recommended scaling factors are $c_1 = 0,3$ and $c_2 = 1,2$. This is called "spin component scaling (SCS)" procedure for MP2 and simply called as SCS-MP2 method [91]. While MP2 generally overestimates the interaction energies because of the equal contributions mentioned above, SCS-MP2 somewhat corrects the results and a lower correlation energy (in absolute value) remains. In most cases, SCS-MP2 underestimates the interaction energies in contrast to MP2.

2.4 Density Functional Theory (DFT)

Density functional theory was developed in 1964 by W.Kohn et. al., with the starting point as electronic density instead of the electronic wavefunction. The main idea behind this theory was that "Does the electronic density has the whole information about a system?". The complete formalism depends on the functions of this density function which are so called as "functionals". However, DFT requires an initial functional to compute the electronic properties and a series of functionals have been developed such as PW91, B3LYP, B3PW91, etc. So, it does not start with the HF theory as the excellent orbital part of the many electron problem. On the other hand, DFT represents the atom as a uniform electron gas, but the atomic electron gas is too nonuniform and also all KS (Kohn-Sham) orbitals (occupied & virtual) are subjected to the same external potential as a result. Although some developments were performed, this problems still hold. It is somewhat problematic in reaction barriers, vdW interactions, H-bonding, excited states, etc.; but more efficient than ab initio ones in terms of computer time and thus available for larger systems which makes it more suitable for MM and MD calculations.

DFT-D was developed to calculate the weak intermolecular interactions. In this method, an empirical dispersion correction term was implemented into DFT procedure to correct the dispersion energy where ordinary DFT fails.

DFT has been combined with SAPT to treat intermolecular forces extensively which is now called as DFT-SAPT [92-96]. It has been reported that the results of this method are very succesfull in weak interactions and comparable with ab initio methods. The main advantage of this method is giving the contributions of different components which are contained in the total interaction. Due to the fact that the SAPT is used in second-order, one only gets the interactions occur up to second-order which are electronic, dispersion, induction, exchange-dispersion and exchange-

induction energies. Thus, that is different from the supermolecular approach. Actually, the original SAPT is computationally more expensive than CCSD(T) method which is the gold standart of today's computational chemistry. DFT-SAPT was developed to response that disadvantage in which the computational cost is reduced by determining the electronic orbital property by DFT, then these properties are implemented into SAPT formalism. But, for the longe-range interactions where the dipole approach is not sufficient, empirical formulae are necessary as the asymptotic corrections.

Recently, the "Density Fitting (DF)" approach was used to develop DF-DFT-SAPT which gives the chance to deal with more complicated systems and their potential energy surfaces in a cheaper and efficient way [97].

2.5 Basis Sets

In 1951, C.C.J.Roothaan wrote the HF equations in the matrix form which is easy to solve by a simple matrix diagonalization (62). But in this sense, there is a coefficient matrix and the coefficients give the wavefunctions as simple linear combinations. This leads one to going through a superposition model for MOs, then each element in the sum is called "basis function". A set of basis functions also known as "basis set". Because of constituting of the molecules from simple atoms, it is very logical to choose these basis functions as the AO functions instead of ordinary mathematical functions (This approximation is also known as LCAO) . Initially, these AOs were the Slater type orbitals (STOs) , but later, F. Boys suggested to write these STOs as the linear combinations of primitive Gaussian functions (GOs) which has the advantage of reducing four centered integrals to two centered ones, etc., supply computational saving. STOs better fit the hydrogenic solutions, but they are difficult to work with in practice. Gaussians give poor description of the shape; but they are computationally more efficient.

There are too many basis sets can be gathered into two main classes as; minimal basis sets and split-valence basis sets. STO-NG type basis sets where an STO is represented by N primitive gaussians are called minimal basis stes. But they are obselete so far because of inaccurate results. In recognition of the fact that valence orbitals are mostly used in computations because of their chemical importance, it is common to represent the valence orbitals particularly better by representing each

valence orbital by more than one basis functions with different zeta parameters. These split-valence ones can be also divided into two classes: Pople basis sets and correlation consistent basis sets. A Pople basis is typically in the form of X-YZ...G; such as 3-21G, 6-31G, etc. In this case, *X* represents the number of primitive Gaussians comprising each core atomic orbital basis function. The *Y* and *Z* indicate that the valence orbitals are composed of two basis functions each, the first one composed of a linear combination of *Y* primitive Gaussian functions, the other composed of a linear combination of *Z* primitive Gaussian functions, etc. (*) represents the polarization functions and (+) for diffuse functions. Correlation consistent (cc-) ones were designed to converge systematically to the complete basis set (CBS) limit using extrapolation techniques. A general cc- basis set can be given as cc-pVNZ; where N is D, T, Q, 5, 6, etc. for corresponding excitations. An aug- suffix (means augmented) is used to add diffuse functions.

It is highly important to note that basis functions are not the atomic orbitals; they are of course chosen to be the easiest mathematical functions in the chemical sense as LCAOs, but one should never forget that it could be possible to use a set of ordinary linearly independent mathematical functions as our basis sets! In other words, one should never assign any physical meaning to these functions. The only chemically meaningful basis is the STO-3G corresponds to a nucleus, an inner shell and a valence shell of electrons.

Additionally, the highly small interaction energies in the quantum world require using of very large basis sets; e.g. for He dimer, the interaction energy between two He atoms can be only computed with a sufficiently large basis set. But again, e.g. a 2h or 1i orbital function used for this He dimer molecule have no physical meaning; they are ordinary mathematical functions for the He ($1s^2$) atom having only two electrons. It was informed that one needs to use a basis set with the highest orbital angular momentum quantum number l=14 to calculate the energy of He ($1s^2$) within 10^{-5} a.u. (58)

2.6 Relativistic Quantum Mechanics

The Quantum Theory that has been builded up first was essentially a non-relativistic one. In the sense of Einstein's "Special Relativity Theory", all physical laws should be Lorentz invariant, independent from the coordinate systems. Newton and

Schrödinger equations are Galilei invariant, but not Lorentz invariant! So, one needs to have a relativistic quantum mechanical wave equation which is invariant under Lorentz transformation. Now, there is a four-component vector which is called the "energy-momentum-4-vector (or simply 4-vector)" contains all the momentum and energy properties of the system; it is the function of three position and a time coordinate (p_1, p_2, p_3; p_0). Time coordinate is about the energy of the system. There is also no need to make the theory conform to "General Relativity" which is required only when one is dealing with gravitation and gravitational forces are quite unimportant in quantum phenomena.

The basic equation of the relativistic quantum mechanics is the Dirac equation, found by P.A.M. Dirac in 1928 (68-76). For a system, in the existence of an external electromagnetic (EM) field, the full Dirac Hamiltonian and the Dirac equation is given as;

$$H = c \,.\, \alpha \,.\, (p - q \,.\, A) + q.\, \phi + \beta.mc^2 \qquad \textbf{(2.17)}$$

$$[c \,.\, \alpha \,.\, (p - q \,.\, A) + q.\, \phi + \beta.mc^2] \,.\, \Psi = E.\, \Psi \qquad \textbf{(2.18)}$$

where A and ϕ are vector and scalar potentials of the EM field respectively; α and β are the 4×4 matrice representations of Hermitian operators defined in terms of Pauli spin matrices.

In Dirac equation, Ψ is an N = 2.(2s+1) component spinor; where (2s+1) spinors for the particle (positive energy solutions) and the second (2s+1) spinors for the anti-particle (negative energy solutions). For the electron, these are called the electronic and positronic solutions. Thus, one should solve a system of equations including N equations. For the electron (s=1/2) we have 4 equations and the wave function is a 4-component spinor: 2 spinors for electron and the remaining two for the positron and there are large and small components of wave function which are 2-component spinors for these solutions:

$$h_D = \begin{bmatrix} E_L & \sigma.p \\ \sigma.p & E_S \end{bmatrix} \qquad \textbf{(2.19)}$$

where large component (ϕ_L) for electronic and small component (ϕ_S) for positronic states:

$$\Psi = \begin{bmatrix} \phi_L \\ \phi_S \end{bmatrix} \quad ; \quad \int_0^{\infty} (\Phi^2_L + \Phi^2_S) \,.\, d\tau = 1 \qquad \textbf{(2.20)}$$

$$E_L = E' + mc^2 \qquad \textbf{(2.21.a)}$$

$$E_S = E' - mc^2 \qquad \textbf{(2.21.b)}$$

In Dirac's relativistic theory, there is not a "node" concept; thus Dirac explains the motion of the particles exactly in contrast to Schrödinger equation which brings about meaningless nodes (71).

In the central (spherically symmetric) field, A=0, $\phi(0) = 0$, and the potential of the field is defined by $V(r) = -e.\phi = -Ze^2/4\pi\varepsilon_o r$ for the electron;

$$H = c \,.\, \alpha \,.\, (-i\hbar\nabla) + \beta.mc^2 - \frac{Ze^2}{4\pi\varepsilon r} \qquad \textbf{(2.22)}$$

is found and for the sake of simplicity, in terms of $E = E' + mc^2$ transformation, one gets the Dirac equation in the υ^2/c^2 (or shortly $Z^2\alpha^2$) approximation by the operator techniques:

$$\left[\frac{p^2}{2m} - \frac{Ze^2}{4\pi\varepsilon r} - \frac{p^4}{8m^3c^2} + \frac{1}{2m^2c^2}\times\frac{1}{r}\times\frac{dV}{dr}\text{L.S} + \frac{\pi\hbar^2}{2m^2c^2}\times\frac{Ze^2}{4\pi\varepsilon r}\times\delta(r)\right].\Phi(r) = E'.\,\Phi(r)$$

First two terms are non-relativistic bare-nuclei Hamiltonian (Schrödinger Hamiltonian), third term is the relativistic kinetic energy correction (mass velocity term), fourth term represents the spin-orbit interaction and the last one is the Darwin term which is completely a quantum mechanical one. Darwin term does not affect to the spin variables and it only exists for l=0, where the spin-orbit interaction is also zero. By solving this equation, one finds the E' eigenvalue, then by adding mc^2, rest energy of the electron, total energy is found.

Dirac equation, which is relativistic and including spin, removes n and l-degeneracy of energy spectrum which was a serious problem in Schrödinger's wave mechanics; but j-degeneracy arises (77).

2.7 Relativistic Quantum Chemistry

The relativistic quantum chemistry arises when one applies the relativistic quantum mechanics to the structure of atoms and molecules. Due to the high velocities of particles comparable with the velocity of light, relativistic effect become important. For Z > 10 atoms and all of the molecules, relativistic effects are quite important and comparable with the correlation energy! For example, the relativistic energy is more than twice as large as the correlation energy for Argon atom (Z=18). The relativistic

effects are also necessary for inner cores where electrons move faster than the outer shells. When Z becomes larger, the relativistic effects become important for valence shells as well (78-81).

Modern electronic structure theory may be viewed as consisting of three parts: HF orbital part, electron correlation part and the relativistic part. There are also some quantum electrodynamical corrections; but they have a small contribution on the energy as to others) For lighter atoms (Z<10), it has been customary to write for the energy of an N-electron system, the terms corresponding to these three parts:

$$E = E_{HF} + E_{corr} + E_{rel} \quad \textbf{(2.24)}$$

But for Z>10 atoms and molecules, this is not true. Relativistic and correlation energies are of comparable magnitude; hence they cannot be separated but; rather, affect each other (46). So, a more general definition is necessary:

$$E = E_{HFD} + E_{rel\text{-}corr} \quad \textbf{(2.25)}$$

where E_{HFD} comes from the Hartree-Fock-Dirac Theory and $E_{rel\text{-}corr}$ is the relativistic correlation energy. Simple Hartree-Fock-Dirac Hamiltonian, without an external field, is given as;

$$H_{HFD} = \sum_{i=1}^{N} h_i^D + \sum_{i>j}^{N} \frac{e^2}{r_{ij}} \quad \textbf{(2.26)}$$

where h_i^D is the one-electron Dirac Hamiltonian. Thus, one concludes that the Hartee-Fock-Dirac Theory treats the one-electro effects relativistically and the electron-electron interactions non-relativistically. But, this is not Lorentz invariant due to the r_{ij} term. To make a complete analysis of electron-electron interactions, one uses the Breit interaction; then the full HFD Hamiltonian is;

$$H_{HFD} = \sum_{i=1}^{N} h_i^D + \sum_{i>j}^{N} g_{ij}^B \quad \textbf{(2.27)}$$

where g_{ij}^B is the Breit interaction including all electron-electron interactions (Coulombic repulsion, spin-orbit, spin-other orbit, orbit-orbit, spin-spin, hyperfine) and two body Darwin term different from the one body Darwin term in the Dirac Hamiltonian (46). This Hamiltoian now, treats the electron-electron interactions relativistically too and generates a wave equation invariant under Lorentz transformation, consistent with special relativity. Thus, we get the full relativistic HF (namely, HFD) theory. But, it still needs some quantum electrodynamical corrections.

2.8 Douglass-Kroll Transformation

The positronic solutions of the Dirac Hamiltonian give rise to equations which are more complicated to interpret physically and more difficult to implement computationally. In Quantum Chemistry, as the quantum mechanics of atoms and molecules, one needs only the electronic solutions (positive energy solutions). Thus, a transformation is required to reduce the coupling between the electronic and positronic solutions;

$$h_D = \begin{bmatrix} E_L & \sigma.p \\ \sigma.p & E_S \end{bmatrix} \quad \textbf{(2.28)}$$

where the diagonal part do not involve interactions between large and small components and the remaining (σ.p) parts describe the interaction between these components. Now, both electronic and positronic solutions are two component solutions.

Exact decoupling of positive and negative energy states (or in other words, the decoupling of large and small components of the wave function) of the Dirac Hamiltonian is possible in the framework of unitary transformation techniques. The resulting two-component Hamiltonians feature exactly the same spectrum of energy eigenvalues as the original Dirac operator. There are three fundamental transformations: Foldy-Wouthuysen, Douglas-Kroll and Barysz-Sadlej-Snijders transformations. Douglas-Kroll transformation can produce an Hamiltonian which is decoupled to a certain order in the fine structure constant (82-85).

As in the common $E(\infty) \rightarrow 0$ reference, the Dirac energy spectrum is first made relative to the rest energy, mc^2; one can perform that operation by substracting mc^2 from the Dirac Hamiltonian:

$$H = c \,.\, \alpha \,.\, p + (\beta - 1) \,.\, mc^2 + V(r) \quad \textbf{(2.29)}$$

(Unfortunately, this operation is generally called “non-relativistic limit”). Now, Douglas-Kroll transformation can be applied to this Hamiltonian. The overall unitary transformation is decomposed as the sequence of sub-unitary transformations:

$$U = \ldots\ldots U_4 U_3 U_2 U_1 U_0 \quad \textbf{(2.30)}$$

Then we get the block diagonal hamiltonian that we want to have;

$$H = U\, H_D\, U^{\dagger} = \begin{bmatrix} h_+ & 0 \\ 0 & h_- \end{bmatrix} \quad \textbf{(2.31)}$$

where ($N_L \times N_L$) dimensional h_+ for electronic and ($N_S \times N_S$) dimensional h_ for positronic states.

First, U_0 is chosen as the Foldy-Wouthuysen transformation for the initial transformation of Douglas-Kroll procedure:

$$H_1 = U_0 H_D U_0^\dagger \quad \textbf{(2.32)}$$

$$H = \ldots\ldots U_2 U_1 H_1 U_1^\dagger U_2^\dagger \ldots\ldots = \begin{bmatrix} h_+ & 0 \\ 0 & h_- \end{bmatrix} \quad \textbf{(2.33)}$$

Thus, we have the electronic and positronic states which were decoupled and the spectrum of that is the same with the original Dirac Hamiltonian as a consequence of unitary transformations. Now, one can solve the electronic part independently which is necessary to treat the atomic and molecular structures.

This Douglas-Kroll Hamiltonian can be written as the sum of the same terms in the Dirac Hamiltonian; non-relativistic term (Schrödinger type), mass-velocity, spin-orbit and Darwin terms. Thus, it is possible to go beyond the non-relativistic solution with three kind of relativistic corrections where mass velocity contribution is always negative in contrast to positive Darwin and spin-orbit energy contributions. Due to the fact that the mass-velocity term makes the largest contribution to the energy when the spin-orbit interaction is the smallest one, then the total energy contribution is always negative which remains the non-relativistic energy levels to slightly lower ones.

Foldy-Wouthuysen and Douglas-Kroll transformations have analytical forms in contrast to Barysz-Sadlej-Snijders numerical one which needs to be solved iteratively and controlled by the convergence of solutions.

In the common sense, the interaction between electron spin and angular momentums with the external electrical and magnetic fields are treated by QED (Quantum Electrodynamics) except from the other terms in Breit equation. There are also some other quantum electrodynamical effects additional to the Breit interaction. Lamb shift is the most important one of these effects and it has always a positive value. For Z>10 atoms, the Lamb shift becomes important; e.g. for Argon atom, the magnitude of the Lamb shift is 0,0552 a.u., comparable to the chemical accuracy limit (≈ 0,0037 a.u.). This effect also removes the j-degeneracy of the Dirac energy spectrum; thus QED corrections are necessary to get the accurate energy spectrum of matter (86, 87).

3. RESULTS AND DISCUSSION

3.1 Pyrazine Dimers

In the sense of the studies in the literature and by depending on our chemical point of view, we have examined ten different configurations for pyrazine dimer in which there is a weak interaction as a sum of CH/π, N/π and π/π interactions. Each structure was confirmed as a stable structure corresponding to a minimum point on the potential energy surface (PES). A computer code so-called PHYTON (108) script has been written to generate all possible structures for pyrazine dimer. The script has created approximately 3000 different conformers. Among them, 10 conformers (Table 3) have been chosen in such a way that

- some of the the conformers were reported as being the conformers with low energy in the literature,
- the conformers involved the appreciable amount of CH/π, N/π and π/π type interactions,
- the distance between the hydrogen atoms of the monomers did not exceed 1.5 Å,
- in-plane and out of plane, parallel and perpendicular rings were considered.

The model structure used in the PYTHON script was given in Fig. 5.

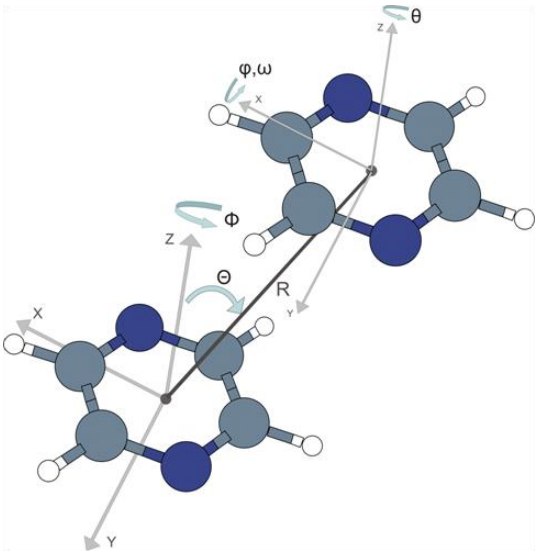

Figure 5 : The model of pyrazine dimer used in the PHYTON script

In Fig. 5, R is the center of mass distance and theta and phi are the polar angles of the line joining the two center of masses with respect to a pyrazine-fixed coordinate system. Then the second pyrazine monomer is rotated using three euler angles. The first rotation is responsible for the angle "phi" about the z-axis, the second rotation for the angle "theta" about the x-axis and the third rotation is responsible for the angle "psi" about the z-axis. So that, there are 6 dimensions in total.

The non-bonded interactions between the pyrazine monomers are rather weak interactions and they can only be treated with very accurate methods. In this study, two approaches were used for this purpose:

Two different conceptual approaches were examined to investigate the interactions between two pyrazine dimers:

- Supermolecular approach
- SAPT approach

In the supermolecular approach, the difference between the total energy of isolated monomers and the energy of dimer is calculated, then the resulting energy is the interaction energy:

$$\Delta E = E_{AB} - E_A - E_B \quad \textbf{(3.1)}$$

A BSSE correction is strongly required in supermolecular calculations due to the fact that we used very large basis sets as aug-cc-pVDZ and aug-cc-pVTZ to treat these weak interactions rigorously. Thus, counterpoise (CP) correction was performed in all calculations:

$$\Delta E = E_{AB} - E_A(AB) - E_B(AB) \quad \textbf{(3.2)}$$

In our supermolecular calculations, MP2, SCS-MP2, DFT-D and CCSD(T) methods were used. In the DFT-D method, B3LYP hybrid functional was chosen, because of the existence of some fairly good results in the literature.

Ten structures, which were found most important to investigate, are shown in Table 2.

Table 2 : Studied conformers of the pyrazine dimer

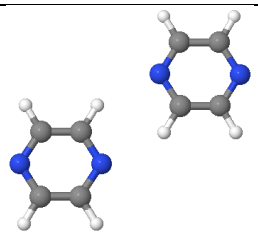	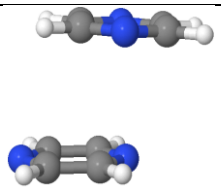
Structure **A** // both rings in the xy-plan, mainly CH----N interaction or classical H-bond	Structure **B** // parallel rings along the z-axis, mainly π-π interaction and also N..π and CH---π interactions
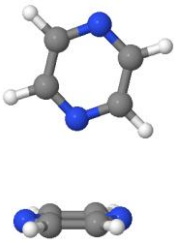	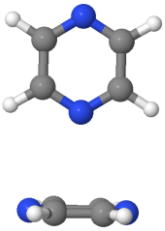
Structure **C** //one ring in the xy-plane, the other is tilted along z-axis, mainly N…π interaction	Structure **D** // one ring in the xy-plane, the other is along z-axis, mainly N…π interaction
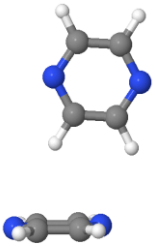	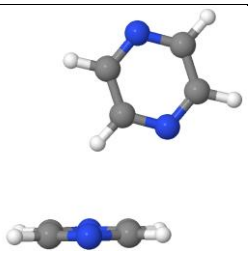
Structure **E** // one ring in the xy-plane, the other is along z-axis, mainly CH----π interaction	Structure **F** // one ring in the xy-plane, the other is tilted along z-axis, mainly CH…π interaction
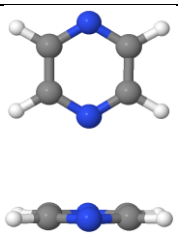	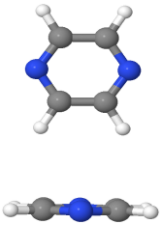
Structure **G** // one ring in the xy-plane, the other is along z-axis, mainly N…π interaction	Structure **H** // one ring in the xy-plane, the other is along z-axis, mainly CH…π interaction
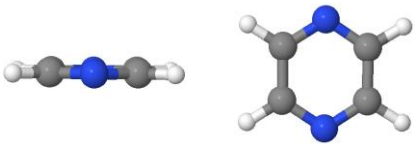	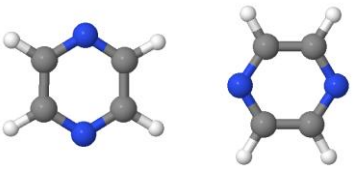
Structure **I** // one ring in the xy-plane, the other is along z-axis, mainly CH----π interaction	Structure **J** // both rings in the xy-plane with non-parallel nitrogens, mainly CH--N interaction or classical H-bond

First, all these configurations have been optimized by MP2, SCS-MP2 and CP corrected SCS-MP2 methods separately in TURBOMOLE program package (107). We used aug-cc-pVDZ basis set in all optimization processes. All these optimizations were performed for each one to prepare them to the interaction energy calculation step. Then, these CP-SCS-MP2 optimized structures have been used in the MOLPRO program package (106) to calculate interaction energies with MP2, SCS-MP2, B3LYP-D DFT-SAPT and CCSD(T) methods. The resulting interaction energies were given in the Table 3.

Table 3 : The interaction energies with different methods (in kJ/mol)

Structure	MP2	SCS-MP2	B3LYP-D	DFT-SAPT	CCSD(T)
A	-17.79	-14.52	-19.06	-13.73	-16.19
B	-25.57	-16.18	-15.66	-12.32	-13.91
C	-17.56	-11.48	-13.06	-9.29	-12.16
D	-17.31	-11.12	-12.20	-8.94	-11.76
E	-13.30	-8.76	-12.14	-8.19	-9.88
F	-13.49	-9.07	-11.48	-8.20	-9.92
G	-11.08	-5.77	-6.16	-3.92	-6.70
H	-8.72	-5.32	-7.38	-5.14	-6.34
I	-2.84	-0.68	-3.24	-0.80	-2.16
J	-10.67	-8.13	-10.75	-7.60	-9.63

These results were also given in the Fig. 6 to make comparison with each other.

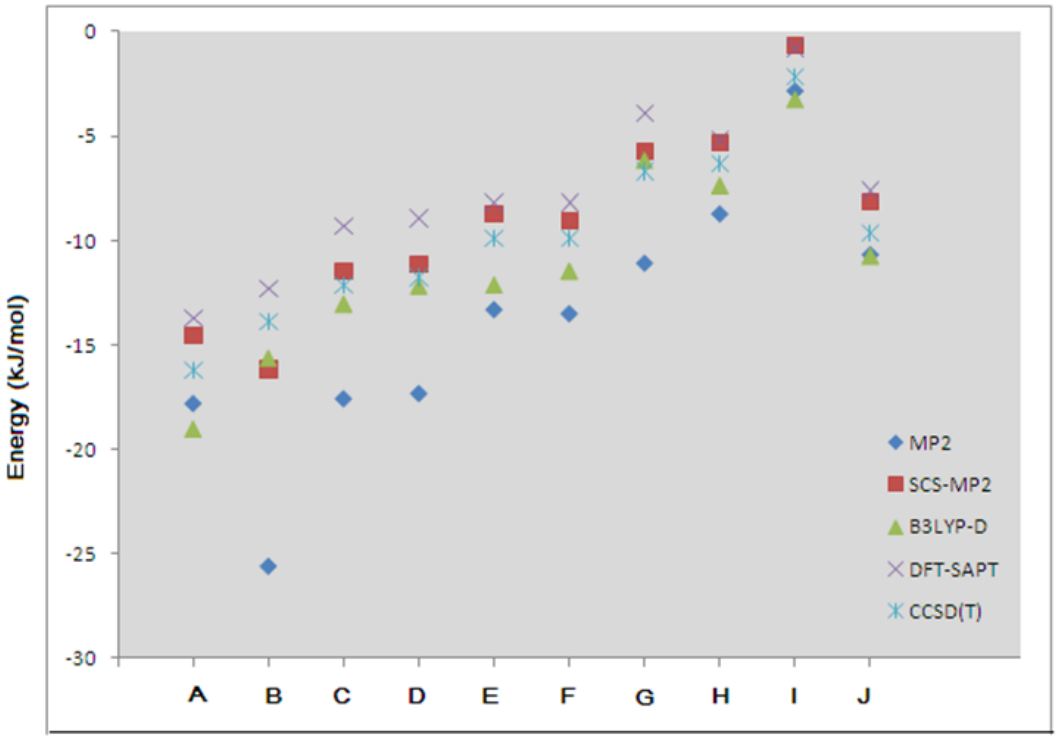

Figure 6 : The interaction energies of conformers in different level of calculations

If we have a glance on the Fig. 6, it can be concluded that doubly-bridged structure A is the most stable configuration for pyrazine dimer; namely it is the global minimum according to CCSD(T) result as the most accurate method. Cross displaced stacked structure B and T-shaped structures C and D are second, third and fourth most stable conformers respectively. The resulting stability order can be given as;

A > B > C > D > F > E > J > G > H > I

If we analyze the total interaction in each structure by comparison, there remains some results as;

- MP2 and B3LYP-D methods overestimate the total interaction energy relative to CCSD(T) results while DFT-D and SCS-MP2 make an underestimation.

-B3LYP-D gives fairly good results in comparison to CCSD(T) method. The accuracy of this method results from the empirical dispersion energy correction implemented into it.

- In structure G, the main contribution to total interaction comes from N/π interaction. CH/π and π/π interactions are expected to be less dominant than NH/π respectively. H structure, which resembles to the G structure, has dominantly CH/π interaction than N/π and π/π. In figure 6, G structure seems to be more stable than H, thus it can be concluded that N/π interaction is a bit stronger than CH/π interaction. Similar situations are valid between E/F and C/D pairs as well. Additionally, a simple comparison between D and E structures also supports that result.

- The reason for the highest stability of structure A is that it has two strong classical N/H hydrogen bond type contacts. B structure is also very stable due to the existence of high population of all three kind of interactions as CH/π, N/π and π/π. It has the richest structure in terms of these interactions among C to J. Structure I is the poorest one in terms of the interaction because it has not a direct N/π, CH/π or π/π interaction. It has the lowest interaction energy and is being stabilized by very longe range CH/π type dispersion forces.

- Due to the fact that the leading intermolecular force is of electrostatic interaction in structure A which has the smallest dispersion type interactions, the dispersion corrected B3LYP-D method gives the worst result for this conformer.

- The dispersion correction in B3LYP-D method works best when the range of dispersion interaction increases; e.g., C, D and G structures support such kind of conclusion.

- MP2 gives the highest overestimation when classical N/H bonding population is somewhat increased; e.g., C, D and especially G structure.

- DFT-SAPT works best for the structures including precised dispersion interaction such as E, F and H. It is not surprising that the dispersion interaction is generally the leading component of SAPT calculations for weak intermolecular forces.

Kleinermanns *et al*. (14) have predicted the A and B structures as the most stable respectively, but in their calculations, for D structure, geometry optimization did not converge to a stable structure, in contrast we have found the converged structure for

D. They have also not performed a BSSE correction to their results which is vitally necessary in such cases. In addition, we performed CCSD(T) calculations for both aug-cc-pVDZ and aug-cc-pVTZ basis sets which is absent in their study. Therefore, our results are computationally more accurate and reliable.

For A and D structures, we have also calculated the same interaction energies with MP2 and SCS-MP2 optimized geometries in comparison to CP-corrected SCS-MP2 ones, Table 4.

Table 4 : Interaction energies with MP2 and SCS-MP2 optimized geometries of A and D structures in different levels of calculations (1 and 2 represents the MP2 and SCS-MP2 optimized geometries respectively) (in kJ/mol)

Structure	**MP2_1**	**MP2_2**	**SCS-MP2_1**	**SCS-MP2_2**	**CCSD(T)_1**	**CCSD(T)_2**
A	-17,36	-17,66	-13,52	-14,20	-15,42	-15,95
D	-16,31	-17,23	-8,52	-10,53	-9,07	-11,14

According to these results, CP-corrected geometries give substantially better results than MP2 and SCS-MP2 geometries used in the calculations. It can be concluded that the interaction energies calculated using the CP-corrected SCS-MP2 geometries converge to a reliable value, that's why we have used these geometries in our all calculations.

All the results can also be given as relative to the interaction energy of global minimum A in comparison, Table 5.

Table 5 : The relative energies of conformers at different level of calculations (in kJ/mol)

Structure	MP2	SCS-MP2	B3LYP-D	DFT-SAPT	CCSD(T)
A	0.0	0.0	0.0	0.0	0.0
B	-7.78	1.66	3.40	1.41	2.28
C	0.23	3.04	6.00	4.44	4.03
D	0.48	3.40	6.86	4.79	4.43
E	4.49	5.76	6.92	5.54	6.31
F	4.30	5.45	7.58	5.53	6.27
G	6.71	8.75	12.9	9.81	9.49
H	9.07	9.2	11.68	8.59	9.85
I	14.95	13.84	15.82	12.93	14.03
J	7.12	6.39	8.31	6.13	6.56

If we have a glance on Table 5, it is clear to see that MP2 substantially overestimates the structure B as the global minimum. But, the other results are consistent with the CCSD(T) sequence. Structure I is also so poor in terms of this weak interaction among all the other structures.

In the SAPT approach, the energy components of the total interaction are found separately as dispersion, electrostatic, exchange-dispersion and exchange-induction energies. The results are not BSSE corrected because of that BSSE is not defined in DFT-SAPT method. Graphs of the different energy components for structures A, B, D and H were shown in Fig. 7, 8, 9 and 10.

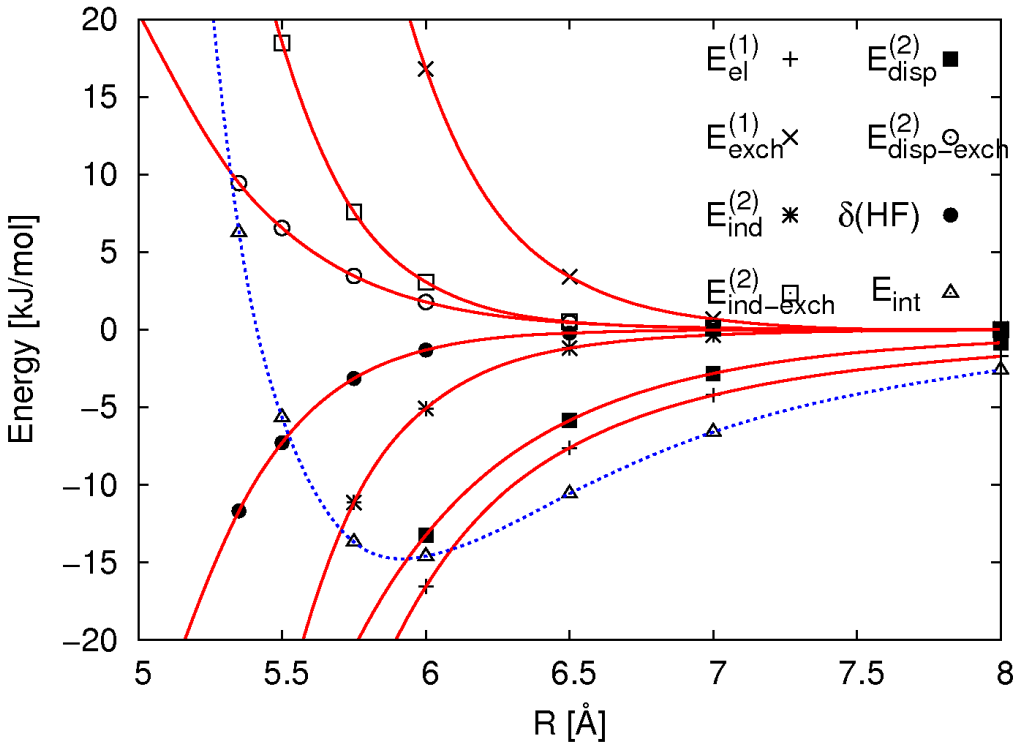

Figure 7 : DFT-SAPT(PBE0AC) energy contributions for the doubly bridged A orientation. Long dashed line E_{int}.

For doubly bridged structure A, electrostatic energy displays the dominant effect to total interaction, dispersion and induction contributions are important as well at short range. At longe range, the contributions of these three energy components changes in the same order with still an electrostatic character.

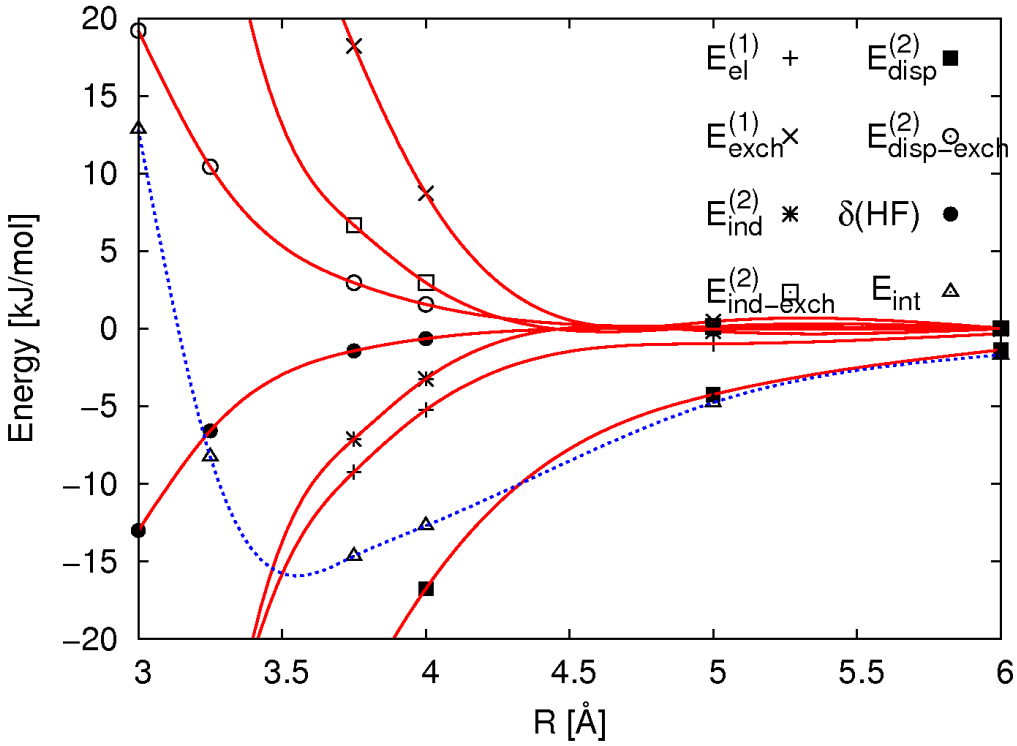

Figure 8 : DFT-SAPT(PBE0AC) energy contributions for the cross-displaced stacked B orientation. Long dashed line E_{int}.

For the cross displaced stacked conformer B, the main contibution comes from the dispersion interaction with the following electrostatic and induction type contributions at short range.

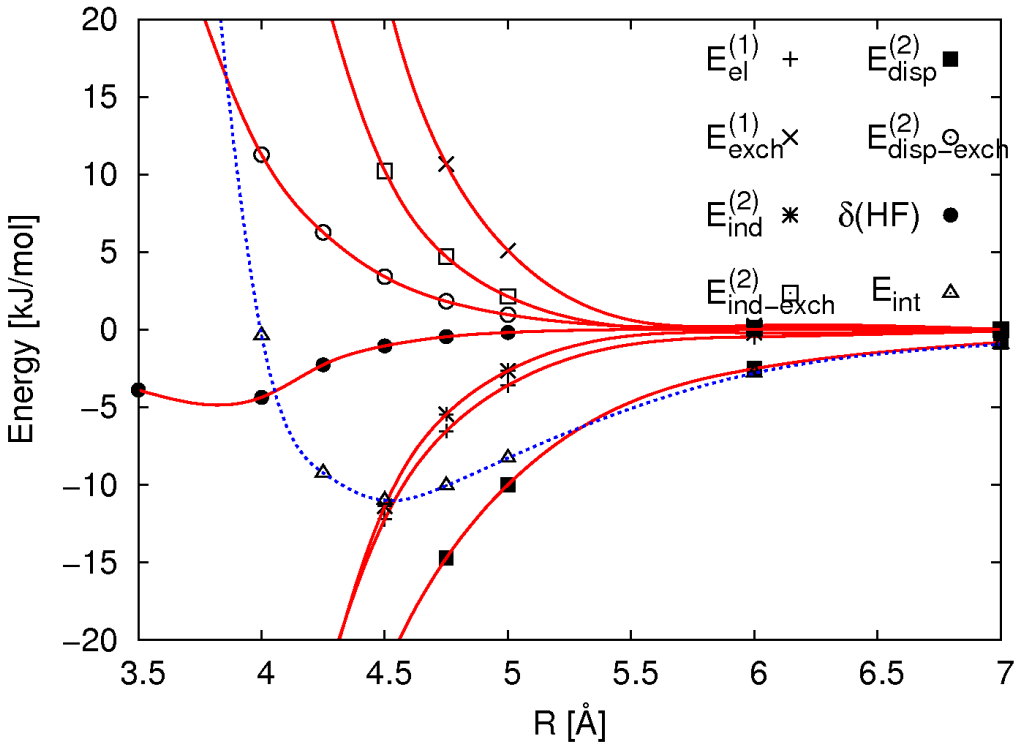

Figure 9 : DFT-SAPT(PBE0AC) energy contributions for the T-shaped D orientation. Long dashed line E_{int}.

In the T-shaped D structure, there is a strong N…π interaction which is the reason for the dominant electrostatic contribution at short range with a following induction energy. But at long range, dispersion interaction starts to get stronger.

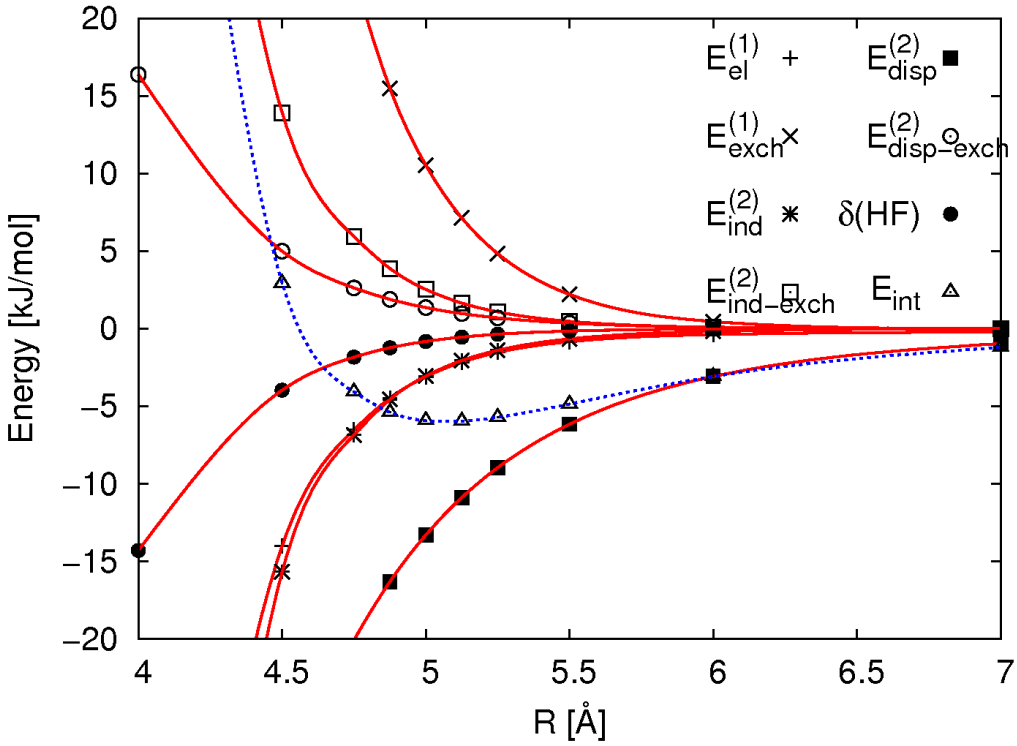

Figure 10 : DFT-SAPT(PBE0AC) energy contributions for H orientation. Long dashed line E_{int}.

For H structure in which the CH…π interaction makes the main contribution to total interaction, dispersion effect has the biggest importance with a following induction contribution. In this structure, electrostatic interaction is less important among these three at short range. At long range, electrostatic energy gets higher in energy up to the same level with induction energy.

The same calculations were also performed with aug-cc-pVTZ basis set to get netter results; Table 6.

Table 6 : The interaction energies in aug-cc-pVTZ basis (in kJ/mol)

Structure	MP2	SCS-MP2	B3LYP-D	DFT-SAPT
A	-19.15	-15.81	-19.01	-14.68
B	-27.98	-18.19	-16.18	-14.27
C	-19.03	-12.73	-13.39	-10.88
D	-18.78	-12.37	-12.53	-10.56
E	-14.75	-10.03	-12.34	-9.18
F	-14.90	-10.28	-11.57	-8.20
G	-12.16	-6.66	-6.57	-5.29
H	-9.73	-6.21	-7.52	-5.14
I	-3.45	-1.21	-3.28	-1.33
J	-11.46	-8.83	-10.75	-7.60

It is clear to conclude that interaction energies are found as slightly higher in aug-cc-pVTZ basis. Specially, DFT-SAPT method displays the highest change for B, C and D structures in which both electrostatic and dispersion interactions are more precised. This result is in also close aggreement with the quality of DFT-SAPT for which we have mentioned above.

Four structures (A, B, D and H) were chosen to investigate their potential energy curves with respect to the intermolecular R distance which is simply the difference between center of masses of monomers. A PEC-R scan was performed for each of these structures in each level of calculation in aug-cc-pVTZ basis. The results were given in Fig. 11, 12, 13 and 14.

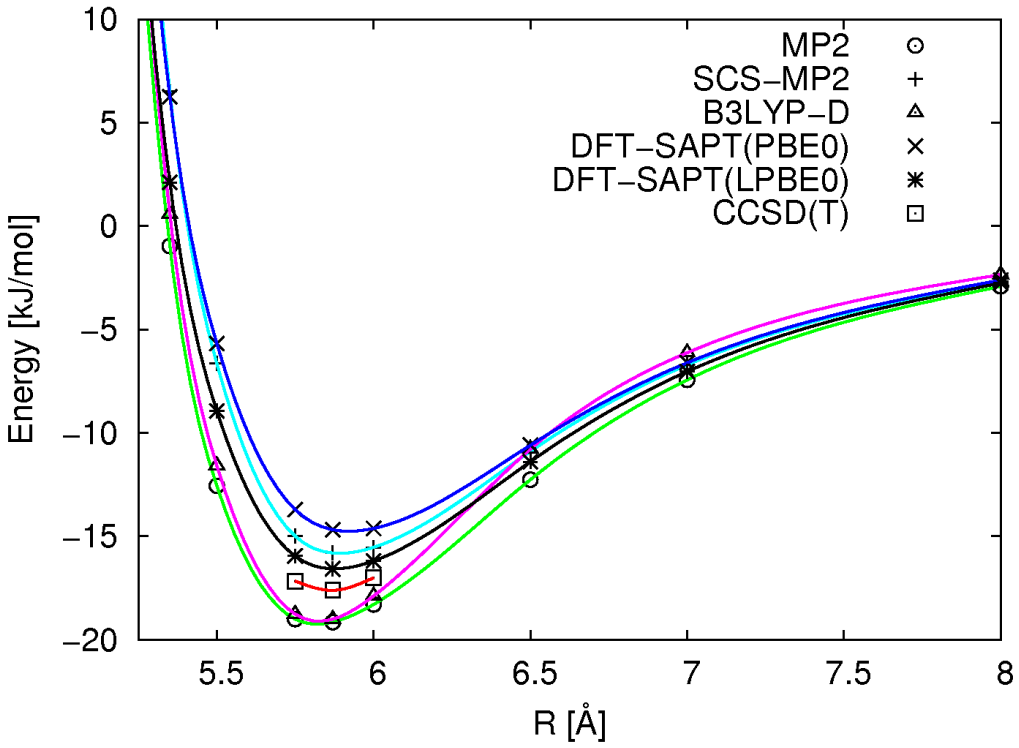

Figure 11 : Potential energy curves obtained from MP2 (green line), SCS-MP2 (cyan line), B3LYP-D (pink line), DFT-SAPT (PBE0AC) (blue line), DFT-SAPT (LPBE0AC) (black line) and CCSD(T) (red line) for the doubly bridged A orientation

In the PEC of structure A, all methods points out the global minimum at the same intermolecular distance in a perfect aggreement.

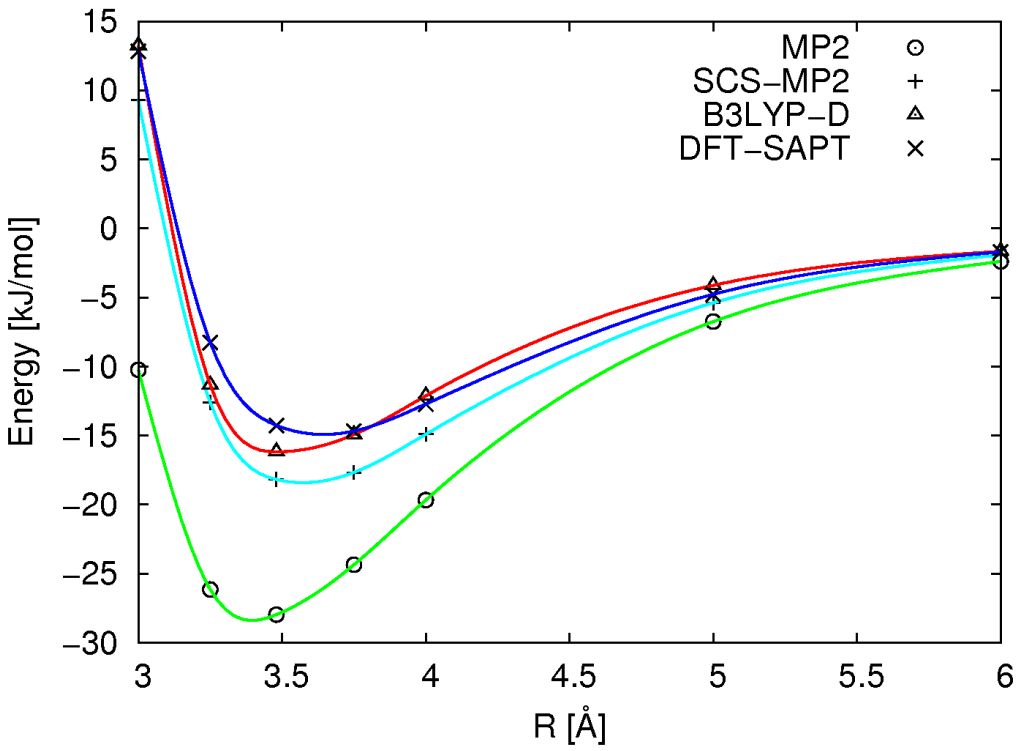

Figure 12 : Potential energy curves obtained from MP2 (green line), SCS-MP2 (cyan line), B3LYP-D (red line) and DFT-SAPT (PBE0AC) (blue line) for the cross displaced stacked B orientation

For the stacked B structure, MP2 and B3LYP predict the global minimum at a different equilibrium distance among the others. DFT-SAPT (PBE0) underestimates the interaction energy.

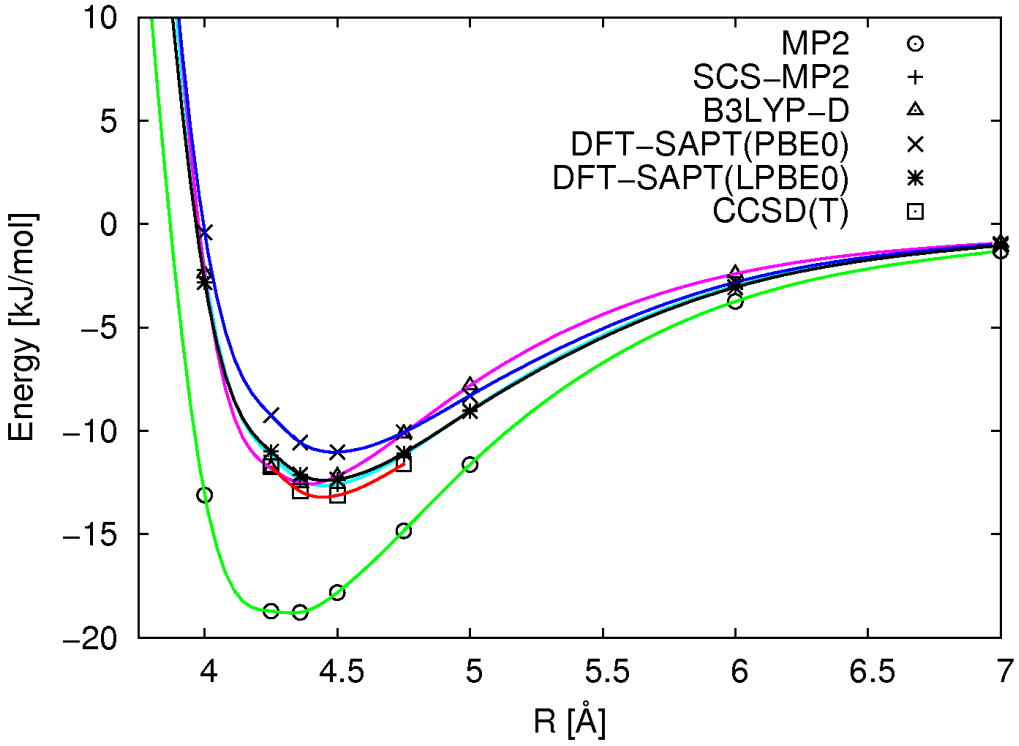

Figure 13 : Potential energy curves obtained from MP2 (green line), SCS-MP2 (cyan line), B3LYP-D (pink line), DFT-SAPT (PBE0AC) (blue line), DFT-SAPT (LPBE0) (black line) and CCSD(T) (red line) for the T-shaped D orientation

B3LYP-D and MP2 methods predict the global minimum differently for the T-shaped D structure in contrast to other methods. SCS-MP2 and DFT-SAPT are well-matched to each other; although these methods underestimate the interaction energy, their minimum structure predictions are more reliable in comparison to CCSD(T).

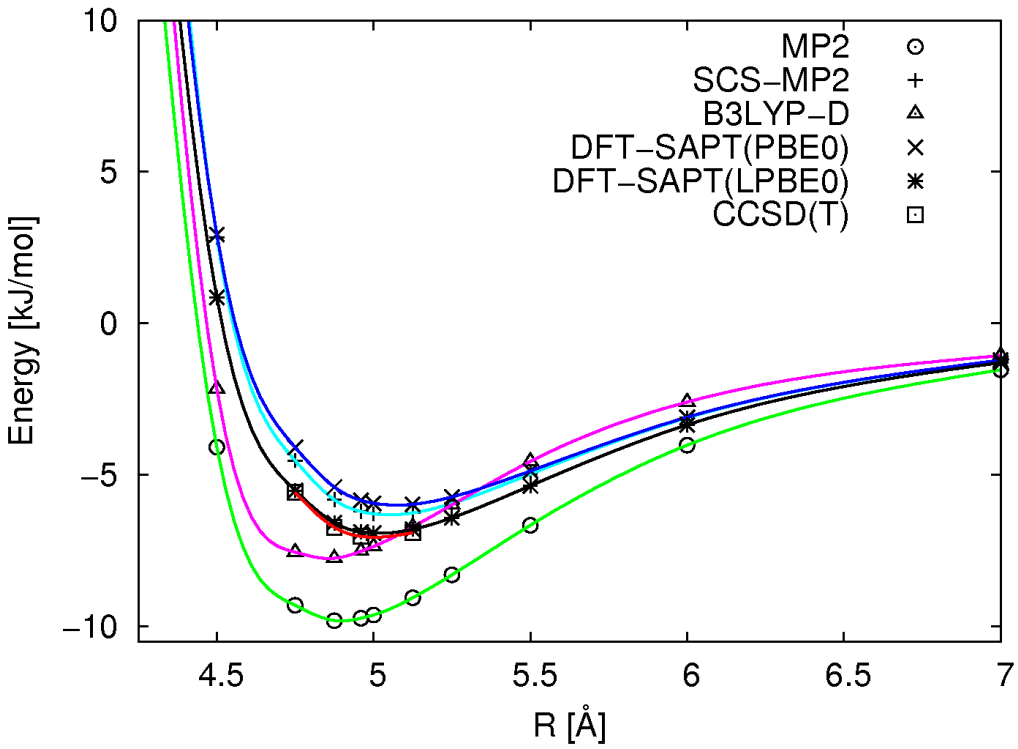

Figure 14 : Potential energy curves obtained from MP2 (green line), SCS-MP2 (cyan line), B3LYP-D (red line) and DFT-SAPT (PBE0AC) (blue line) for the H orientation

B3LYP-D and MP2 again predict the global minimum for H structure slightly at a higher intermolecular distance. SCS-MP2 and DFT-SAPT are still consistent with each other. CCSD(T) matches substantially well with DFT-SAPT (LPBE0) results. DFT-SAPT (PBE0) a bit underestimates the interaction energy.

As a general consequence, it seems that global minimum may have been changed in different methods.

The PEC of stacked B structure was treated in aug-cc-pVDZ level of calculation due to the high population of different interactions and also the lack of symmetry. The PEC of this conformer was given in figure 15.

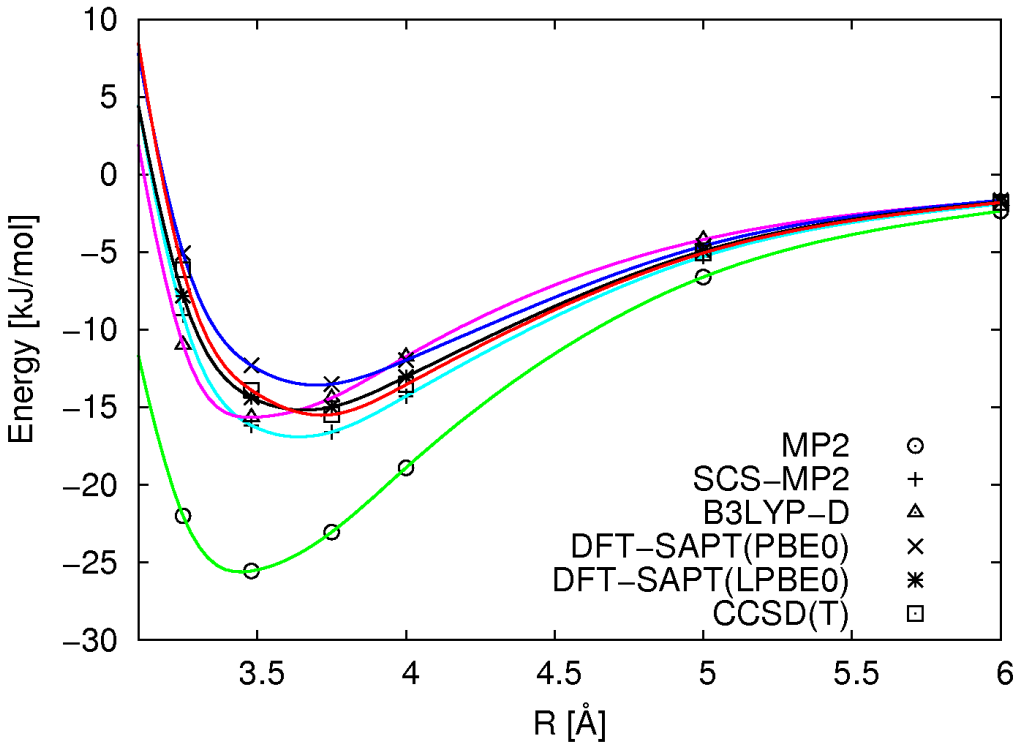

Figure 15 : Potential energy curves obtained from MP2 (green line), SCS-MP2 (cyan line), B3LYP-D (pink line) and DFT-SAPT (PBE0AC) (blue line), DFT-SAPT (LPBE0) (black line) and CCSD(T) (red line) for the B orientation

For the stacked B structure, MP2 and B3LYP-D still predict the global minimum at a different point than the others in aug-cc-pVDZ basis. DFT-SAPT (LPBE0) and CCSD(T) are well-matched to each other. DFT-SAPT (PBE0) still underestimates the interaction energy.

The equilibrium distance (R_{min}) values for each of these structures were given in table 7 with corresponding energy values. The results of B structure correspond to same values in aug-cc-pVDZ level.

Table 7 : The equilibrium distance values of A, B, D and H structures

Method & Structure	R_{min} (Å)	Energy [kJ/mol]
A_MP2	5,831	-19,2440
A_SCS-MP2	5,913	-15,8174
A_B3LYP-D	5,834	-19,1256
A_DFT-SAPT (PBE0)	5,945	-14,8112
A_DFT-SAPT (LPBE0)	5,862	-16,5750
A_CCSD(T)	5,862	-17,6139
B_MP2	3,450	-25,6684
B_SCS-MP2	3,663	-16,9770
B_B3LYP-D	3,468	-15,6767
B_DFT-SAPT (PBE0)	3,697	-13,6711
B_DFT-SAPT (LPBE0)	3,673	-15,2662
B_CCSD(T)	3,700	-15,6683
D_MP2	4,324	-18,8669
D_SCS-MP2	4,464	-12,6545
D_B3LYP-D	4,355	-12,5321
D_DFT-SAPT (PBE0)	4,483	-11,0409
D_DFT-SAPT (LPBE0)	4,466	-12,4035
D_CCSD(T)	4,452	-13,1833
H_MP2	4,871	-9,8112
H_SCS-MP2	5,053	-6,3106
H_B3LYP-D	4,850	-7,7856
H_DFT-SAPT (PBE0)	5,081	-5,9944
H_DFT-SAPT (LPBE0)	4,999	-6,9254
H_CCSD(T)	5,008	-7,0571

It is clear to conclude that, DFT-SAPT and SCS-MP2 work well for all A, B, D and H structures due to the very close values to CCSD(T)-R_{min} result. B3LYP-D underestimates the equilibrium distances in each of them. MP2 substantially underestimates the R_{min} values because of the overestimation of the interaction. Additionally, the closeness of DFT-SAPT (LPBE0) results to CCSD(T) ones is very remarkable.

Relativistic corrections to the energies were also calculated with MOLPRO program package. The relativistic energy of an isolated nitrogen and carbon atoms are -16,94 and -8,65 kcal/mol respectively. Thus, the electronic energies of pyrazine molecule and all its dimer structures should be relativistically corrected. The relativistic energy of an isolated pyrazine molecule was calculated as -69,274 kcal/mol which is comparable to its correlation energy as -532,167 kcal/mol. That results such kind of corrections should not be negligible in real calculations. The same corrections were performed for all dimer structures and it was found that the relativistic energy is almost twice of a pyrazine molecule and nearly the same for all dimers, in the order of -140 kcal/mol which is also comparable their the correlation energies as approximately -549,425 kcal/mol. Therefore, the relativistic effect on these weak interactions are in the order of 10^{-4} a.u. or 0,4 kJ/mol and is negligible.
The different components of the total relativistic energy of pyrazine was shown in Table 8.

Table 8 : The energy components of the total relativistic energy of pyrazine

Darwin term (a.u.)	Mass velocity Term (a.u.)	Spin-orbit Term (a.u.)	Total relativistic energy (a.u.)
0,4725	-0,5890	0,0061	-0,1104

According to the results, the dominant contribution is of mass velocity term which makes the total relativistic energy negative as expected. The same contributions for the dimers were found as twice of the pyrazine monomer again. These results are consistent with the dissociation process of the nitrogen molecule which has also shown the HF orbital wavefunction is sufficient to calculate the relativistic energy except from the spectroscopic work (58), but it still needs some Breit interaction type corrections and also some QED corrections as well.

3.2 Triazine Dimers

Eight different structures, which were found most important to investigate for triazine dimers, are shown in table 9.

Table 9 : Studied conformers of the triazine dimer

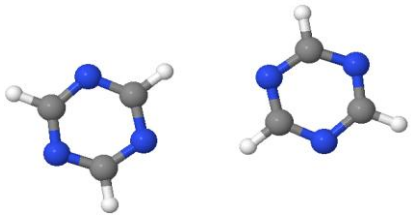	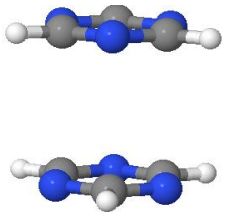
Structure **A** // both rings in the xy-plane, mainly CH----N interaction or classical H-bond	Structure **B** // parallel rings along the z-axis, mainly π-π interaction and also N..π and CH---π interactions
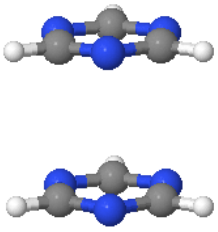	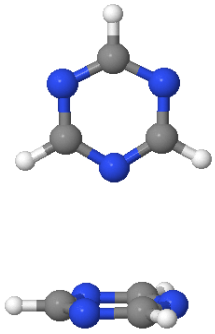
Structure **C** // parallel rings along the z-axis, complete eclipsed rings by atom to atom, mainly π-π interaction and also N..π and CH---π interactions	Structure **D** // one ring in the xy-plane, the other is along z-axis, mainly N…π interaction
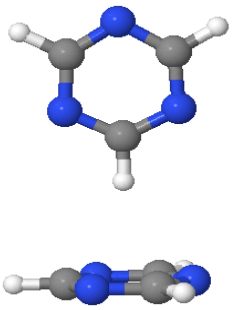	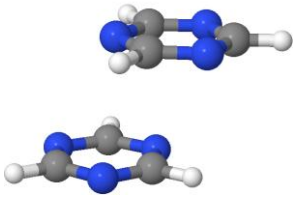
Structure **E** // one ring in the xy-plane, the other is along z-axis, mainly CH----π interaction	Structure **F** // parallel rings along the z-axis, one of two is tilted, mainly π-π interaction and also N..π and CH---π interactions
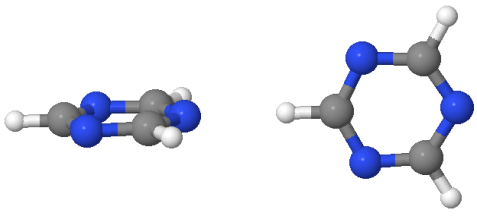	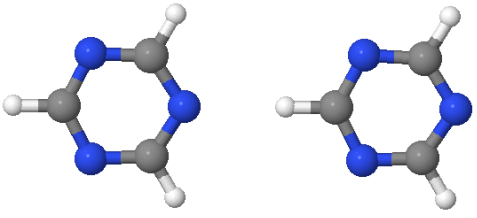
Structure **G** // one ring in the xy-plane, the other is along z-axis, mainly CH...N classical H bond	Structure **H** // both rings in the same plane, mainly CH--N interaction or classical H-bond

First, all these configurations have been optimized by MP2 and CP corrected SCS-MP2 methods separately in TURBOMOLE program package. We used aug-cc-pVDZ basis set in all optimization processes. All these optimizations were performed for each one to prepare them to the interaction energy calculation step. Then, these optimized structures have been used in the MOLPRO program package again -similar to pyrazine- to calculate interaction energies with MP2, SCS-MP2, B3LYP-D DFT-SAPT and CCSD(T) methods. The resulting interaction energies were given in the Table 10.

Table 10 : The interaction energies with different methods (in kJ/mol)

Structure	MP2	SCS-MP2	B3LYP-D	DFT-SAPT	CCSD(T)
A	-15,269	-13,046	-18,260	-13,433	-15,537
B	-19,012	-13,227	-14,752	-12,647	-14,716
C	-10,658	-4,847	-3,910	-2,393	-
D	-15,537	-11,195	-13,340	-10,166	-14,307
E	-9,777	-6,139	-9,282	-4,715	-
F	-21,090	-13,336	-15,705	-11,452	-14,332
G	-8,570	-7,121	-9,894	-6,233	-
H	-9,953	-8,471	-11,421	-7,525	-

These results were also given in the figure 16 to make comparison with each other.

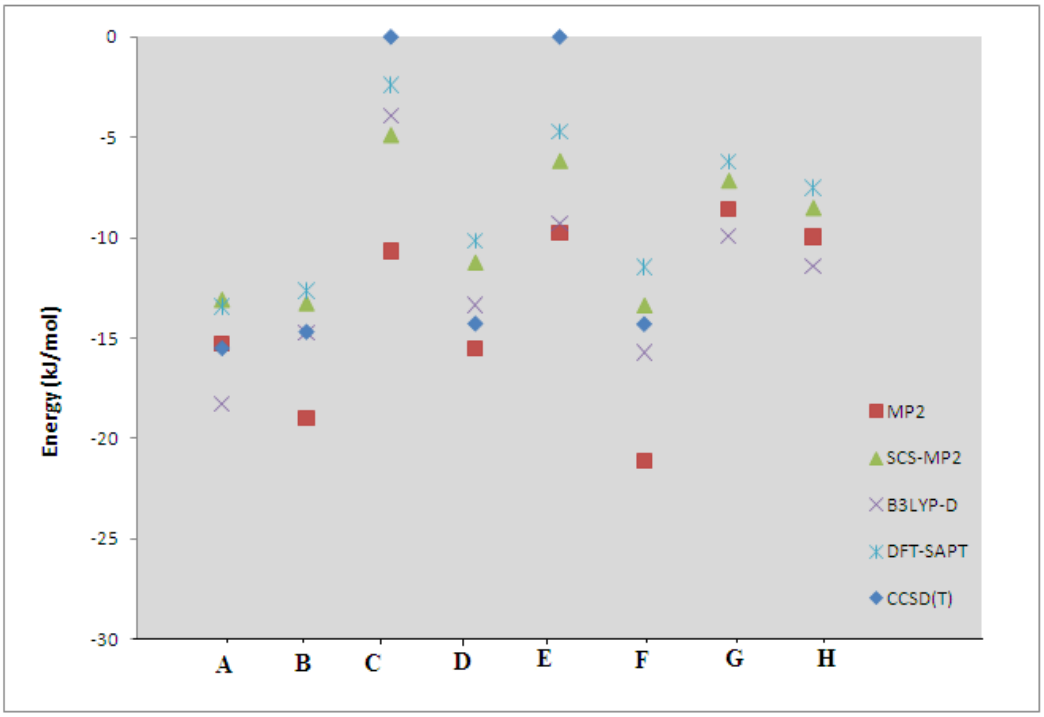

Figure 16 : The interaction energies of conformers in different level of calculations

- The global minimum is found as the doubly-bridged A structure in which classical hydrogen bonding mostly exists. This is also in perfect agreement with the crystal structure of 1,3,5-triazine.

- B and F highly stacked structures are the following most stable local mimimum conformers of 1,3,5-triazine which supports our qualitative predictions about the triazine dimers. Because –as we have said before- unlike the benzene molecule which has a negative electrostatic potential inside the carbon ring, triazines have positive electrostatic potential inside the ring and all the nitrogen including regions outside the ring have negative electrostatic potential, this is the reason for the favoured stacked triazine dimer structures in contrast to T-shaped like benzene dimers.
dimers.

- It is interesting to note that B3LYP-D substantially overestimates the interaction energy in A, G and H structures where classical hydrogen bonding displays the leading role in total interaction.

- In general, DFT-SAPT and SCS-MP2 predict the interaction energies lower than the CCSD(T) results.

- Although one expects a good performance from MP2, it fails in treating the global minimum A in which classical hydrogen bonding exists. Therefore, SCS-MP2 displays a performance parallel to MP2 and highly underestimates the interaction energy.

- B3LYP-D results start to get closer to CCSD(T) ones in the stacked and T-shaped structures in which aromatic hydrogen bond mostly exists.

- DFT-SAPT (PBE0) and SCS-MP2 are well-matched to each other at almost each structure.

- B3LYP-D works well in treating B and C structures where π-π interaction is highly important. It can be attributed to the high dispersion dependence of π-π interaction.

- It can be concluded that, all methods display a problematic treatment of T-shaped D structure which is mainly of N-π interaction. B3LYP-D seems somewhat better among the others in comparison to CCSD(T).

In the SAPT approach, the energy components of the total interaction are found separately as dispersion, electrostatic, exchange-dispersion and exchange-induction energies. Graphs of the different energy components for structures A, B, D and H were shown in Fig. 17, 18, 19 and 20.

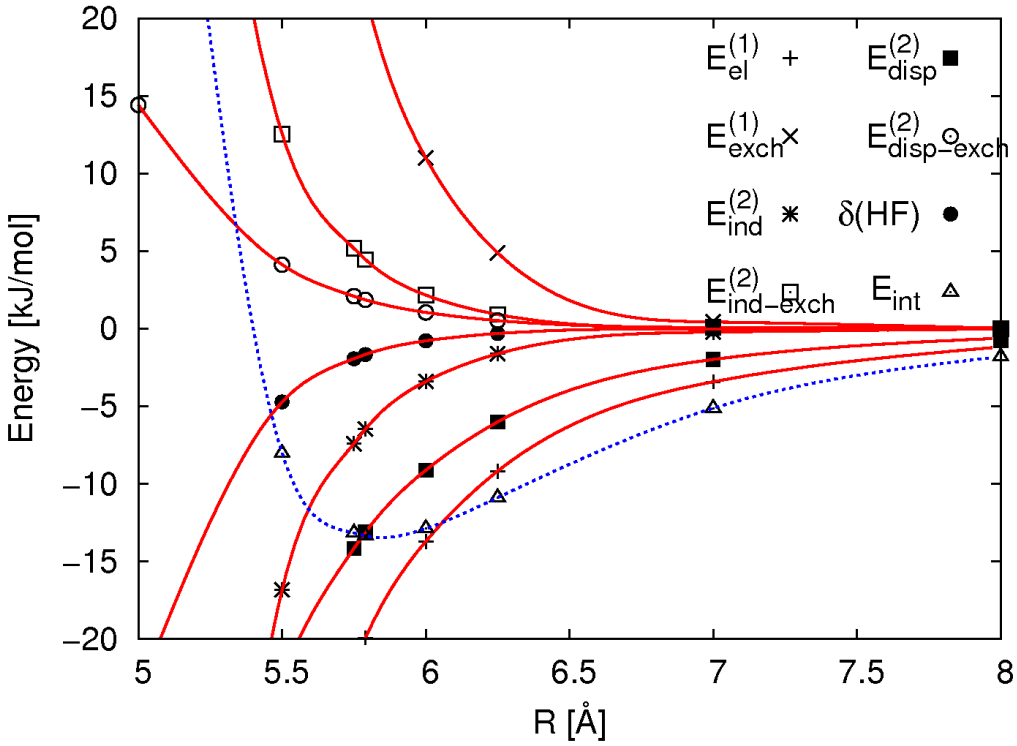

Figure 17 : DFT-SAPT(PBE0AC) energy contributions for the doubly-bridged A orientation. Long dashed line E_{int}

For doubly-bridged structure A, electrostatic energy displays the dominant effect to total interaction, dispersion and induction contributions are important as well at short range. At longe range, the contributions of these three energy components changes in the same order with still an electrostatic character.

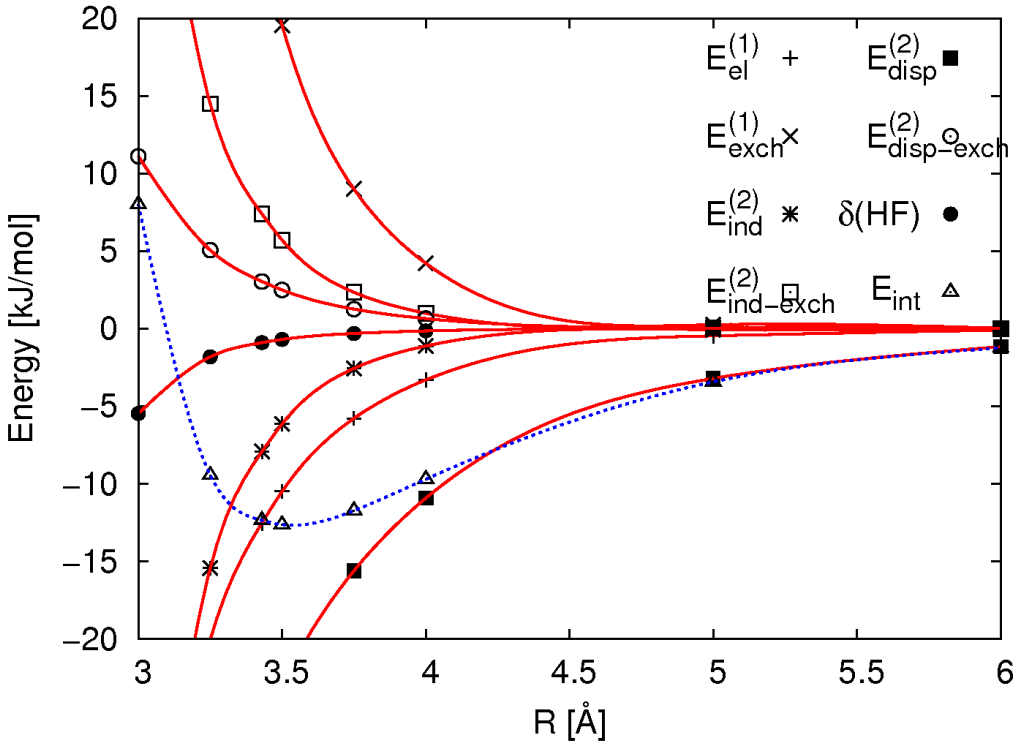

Figure 18 : DFT-SAPT(PBE0AC) energy contributions for the stacked B orientation. Long dashed line E_{int}

For the stacked conformer B, the main contibution comes from the dispersion interaction with the following electrostatic and induction type contributions at short range.

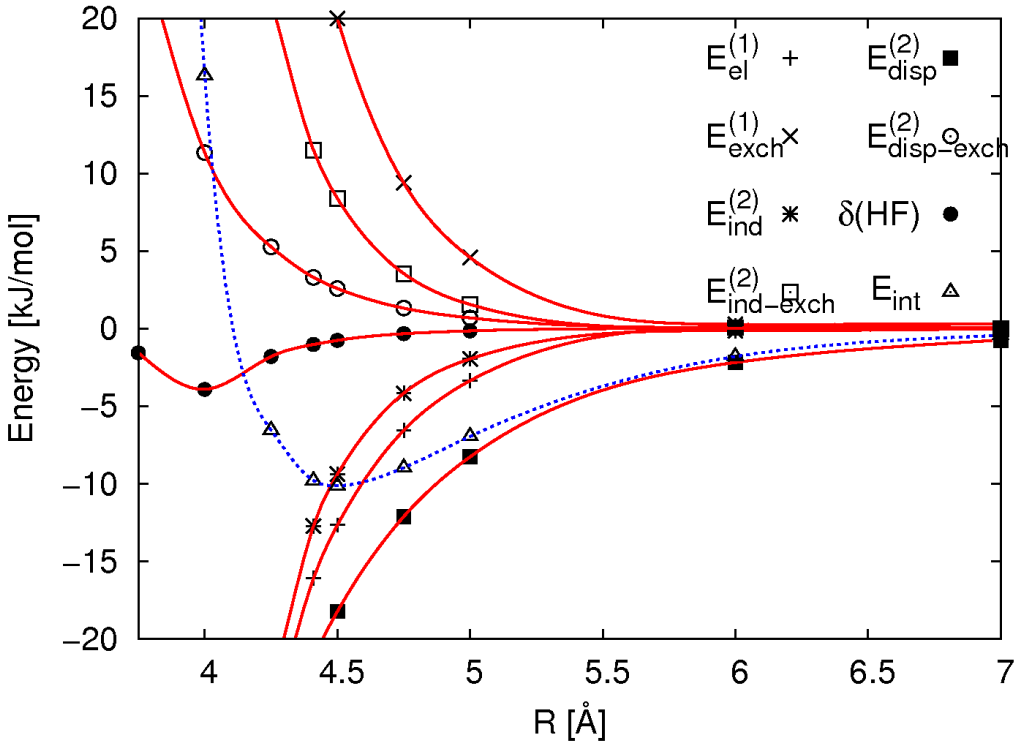

Figure 19 : DFT-SAPT(PBE0AC) energy contributions for the T-shaped D orientation. Long dashed line E_{int}

In the T-shaped D structure, there is a strong N…π interaction which is the reason for the dominant electrostatic contribution at short range with a following induction and dispersion energy. But at long range, dispersion interaction starts to get stronger.

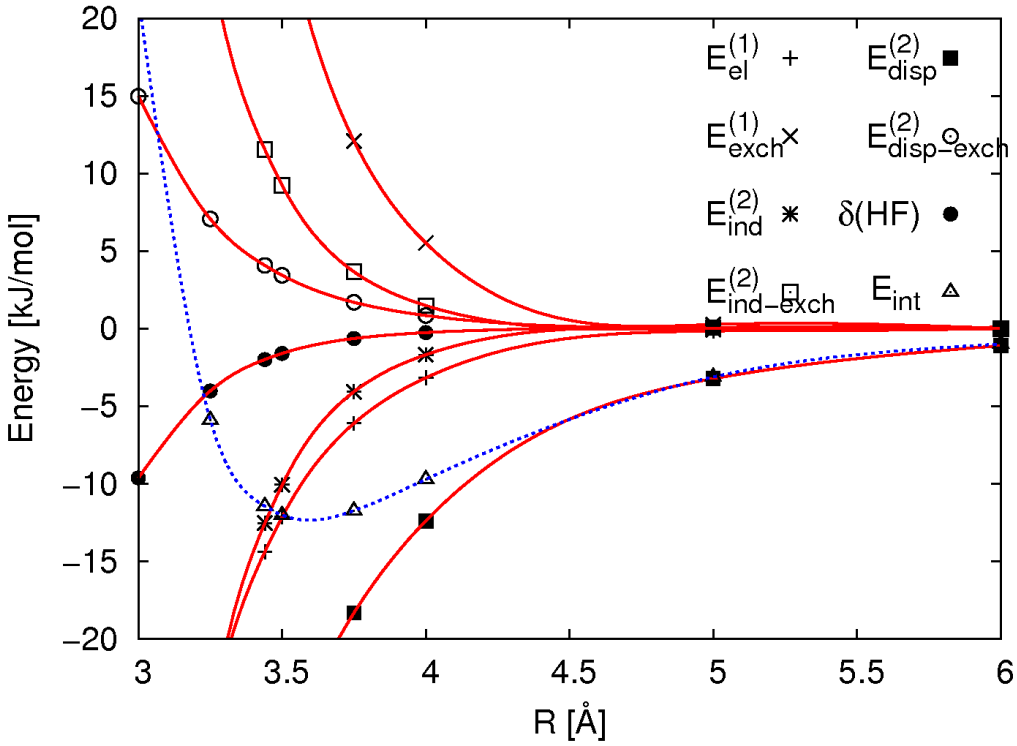

Figure 20 : DFT-SAPT(PBE0AC) energy contributions for the cross-displaced stacked F orientation. Long dashed line E_{int}

For the stacked conformer F, the main contibution comes from the dispersion interaction with the following electrostatic and induction type contributions important at short range.

Four structures (A, B, D and H) were chosen to investigate their potential energy curves with respect to the intermolecular R distance which is simply the difference between center of masses of monomers. A PEC-R scan was performed for each of these structures in each level of calculation in aug-cc-pVDZ basis. The results were given in Fig. 21, 22, 23 and 24.

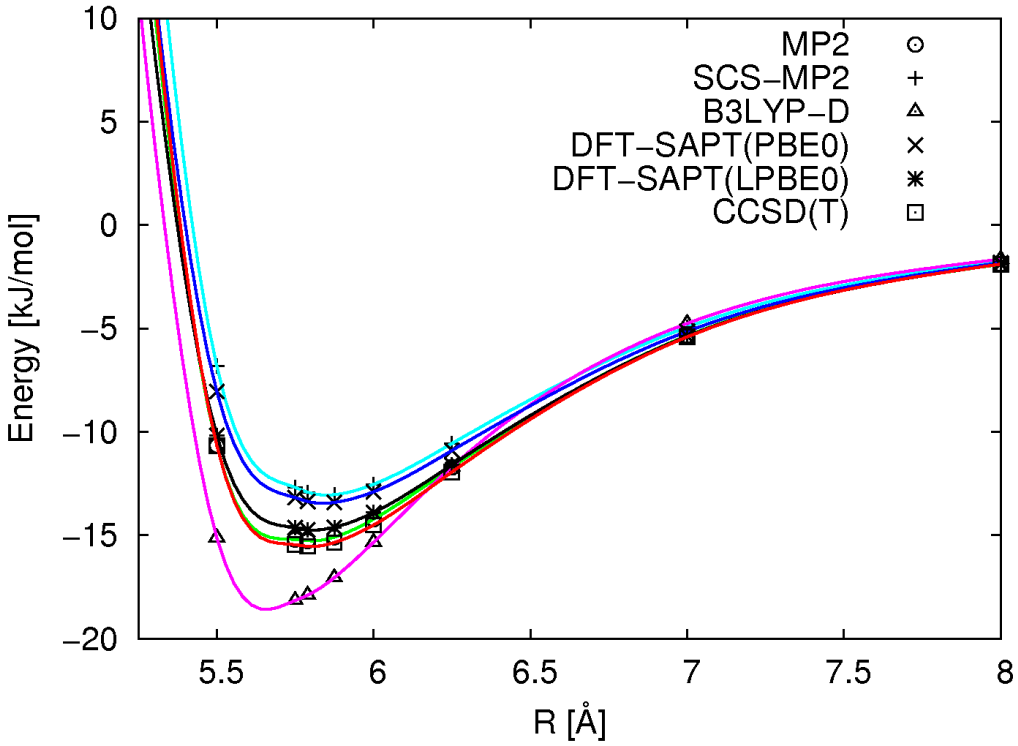

Figure 21 : Potential energy curves obtained from MP2 (green line), SCS-MP2 (cyan line), B3LYP-D (pink line), DFT-SAPT (PBE0AC) (blue line), DFT-SAPT (LPBE0) (black line) and CCSD(T) (red line) for the doubly-bridged A orientation

It is easy to conclude that MP2 works so well in this doubly-bridged A structure because of the existence of classical hydrogen bond. However, the matching between MP2 and CCSD(T) is better than the DFT-SAPT (LPBE0)!

SCS-MP2 and DFT-SAPT (PBE0) are very close to each other as been expected. In both the repulsive and attractive region beyond the equilibrium distance, DFT-SAPT (LPBE0), MP2 and CCSD(T) perform almost equal.

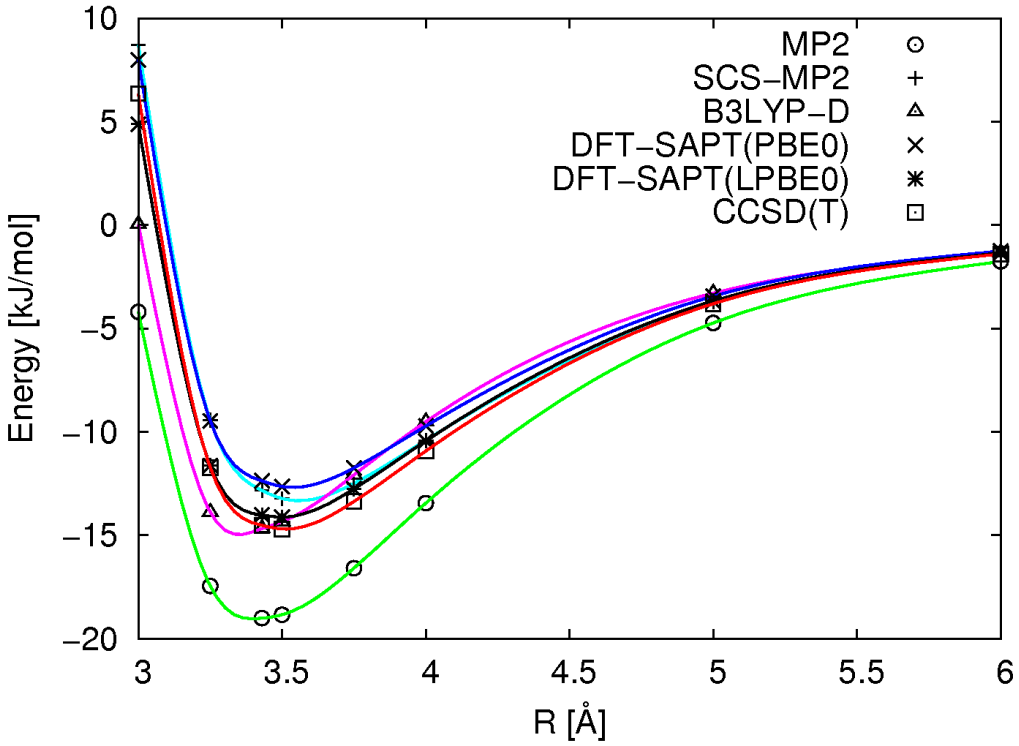

Figure 22 : Potential energy curves obtained from MP2 (green line), SCS-MP2 (cyan line), B3LYP-D (pink line), DFT-SAPT (PBE0AC) (blue line), DFT-SAPT (LPBE0) (black line) and CCSD(T) (red line) for the stacked B orientation

It seems that B3LYP-D predicts the global minimum at a different point among the others. DFT-SAPT (LPBE0) displays the best match with CCSD(T) for this stacked geometry where there is a high population of different kind of interactions.

SCS-MP2 and DFT-SAPT (PBE0) are still close to each other. In the repulsive region, DFT-SAPT (LPBE0) gives equal results with CCSD(T).

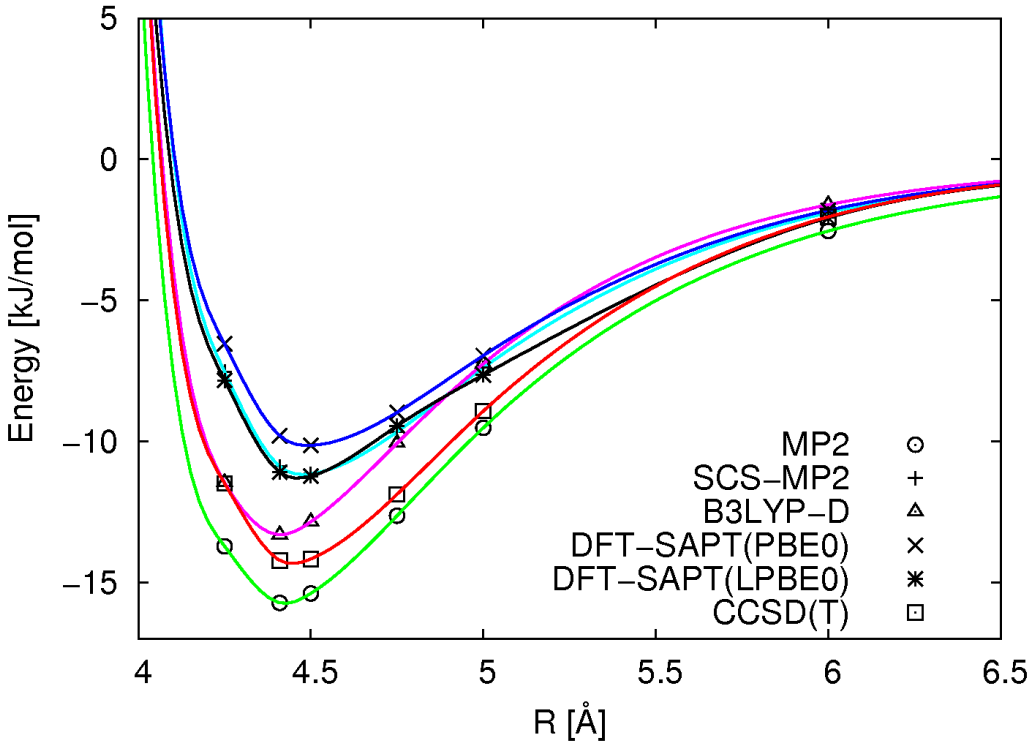

Figure 23 : Potential energy curves obtained from MP2 (green line), SCS-MP2 (cyan line), B3LYP-D (pink line), DFT-SAPT (PBE0AC) (blue line), DFT-SAPT (LPBE0) (black line) and CCSD(T) (red line) for the T-shaped D orientation

It is interesting to conclude that, DFT-SAPT (LPBE0) substantially fails in the treatment of T-shaped D structure. B3LYP-D displays the best fit to CCSD(T) results, especially in the repulsive region. In this structure, DFT-SAPT (LPBE0) performs as good as SCS-MP2 while DFT-SAPT (PBE0) completely fails.

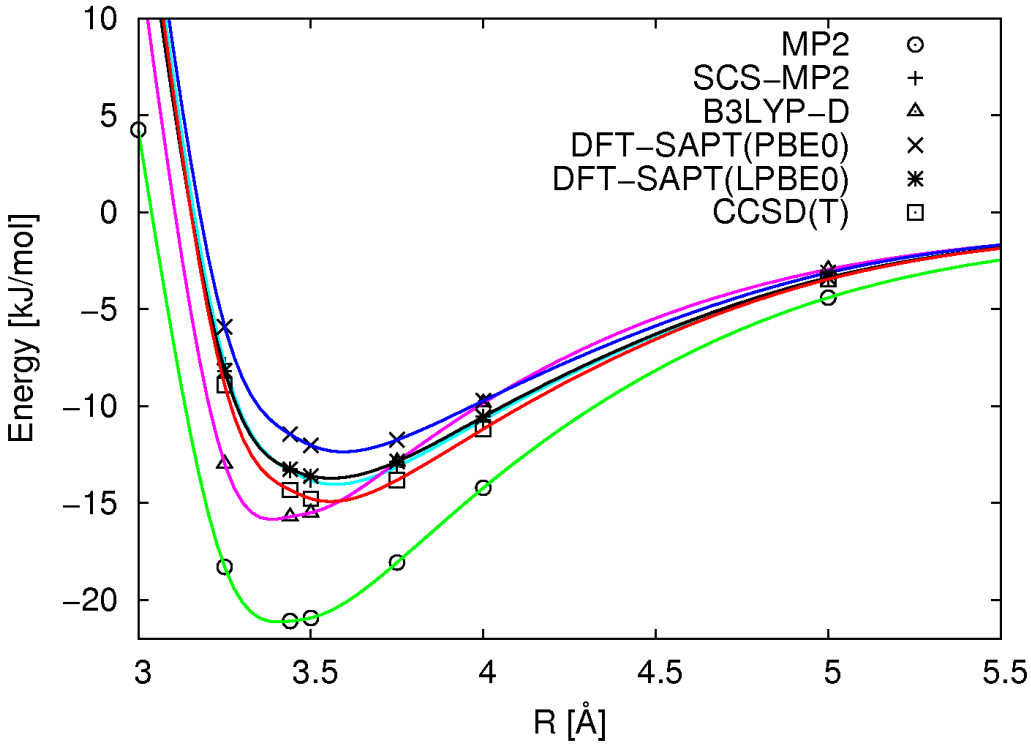

Figure 24 : Potential energy curves obtained from MP2 (green line), SCS-MP2 (cyan line), B3LYP-D (pink line), DFT-SAPT (PBE0AC) (blue line), DFT-SAPT (LPBE0) (black line) and CCSD(T) (red line) for the tilted stacked F orientation

It can be found that, DFT-SAPT (LPBE0) somewhat fails in the treatment of this tilted stacked F structure. B3LYP-D predicts the global minimum at a different point among the others. In this structure, DFT-SAPT (LPBE0) performs as good as SCS-MP2 while DFT-SAPT (PBE0) completely underestimates.

The equilibrium distance (R_{min}) values for each of these structures were given in table 11 with corresponding energy values.

Table 11 : The equilibrium distance values of A, B, D and F structures

Method & Structure	R_{min} (Å)	Energy [kJ/mol]
A_MP2	5.784	-15.2698
A_SCS-MP2	5.859	-13.0463
A_B3LYP-D	5.712	-18.2608
A_DFT-SAPT (PBE0)	5.847	-13.4337
A_DFT-SAPT (LPBE0)	5.787	-14.7343
A_CCSD(T)	5.786	-15.5375
B_MP2	3.421	-19.0120
B_SCS-MP2	3.498	- 13.2275
B_B3LYP-D	3.388	-14.7529
B_DFT-SAPT (PBE0)	3.493	-12.6472
B_DFT-SAPT (LPBE0)	3.483	-14.1533
B_CCSD(T)	3.486	-14.7168
D_MP2	4.403	-15.7361
D_SCS-MP2	4.481	-11.1955
D_B3LYP-D	4.396	-13.3404
D_DFT-SAPT (PBE0)	4.486	-10.1662
D_DFT-SAPT (LPBE0)	4.473	-11.3194
D_CCSD(T)	4.461	-14.3071
F_MP2	3.435	-21.092
F_SCS-MP2	3.500	-13.837
F_B3LYP-D	3.429	-15.716
F_DFT-SAPT (PBE0)	3.613	-12.168
F_DFT-SAPT (LPBE0)	3.496	-13.614
F_CCSD(T)	3.498	-14.782

It is clear to see that, DFT-SAPT (LPBE0) works so well for all structures due to the very close values to CCSD(T)-R_{min} result. SCS-MP2 dispalys a very good performance too in all structures, especially in F. B3LYP-D underestimates the equilibrium distances in each of them. MP2 substantially underestimates the R_{min} values because of the overestimation of the interaction. Additionally, the closeness of DFT-SAPT (LPBE0) results to CCSD(T) ones is highly remarkable.

Relativistic corrections to the energies were also calculated with MOLPRO program package. Due to the very high relativistic energy of an isolated nitrogen and carbon atoms, the electronic energies of triazine molecule and all its dimer structures should be relativistically corrected as in the pyrazine. The relativistic energy of an isolated triazine molecule was calculated as -77,508 kcal/mol which is comparable to its correlation energy as -373,367 kcal/mol. That results such kind of corrections should not be negligible in real calculations. The same corrections were performed for all dimer structures and it was found that the relativistic energy is almost twice of a triazine molecule and nearly the same for all dimers, in the order of -154 kcal/mol which is also comparable their the correlation energies as approximately -559,631 kcal/mol. Therefore, the relativistic effect on these weak interactions are again in the order of 10^{-4} a.u. or 0,4 kJ/mol and is negligible.

The different components of the total relativistic energy of triazine was shown in Table 12.

Table 12 : The energy components of the total relativistic energy of triazine

Darwin term (a.u.)	Mass velocity Term (a.u.)	Spin-orbit Term (a.u.)	Total relativistic energy (a.u.)
0.5266	-0.6572	0.0071	-0.1235

According to the results, the dominant contribution is of mass velocity term which makes the total relativistic energy negative as expected. The same contributions for the dimers were found as twice of the triazine monomer again. These results are still consistent with the dissociation process of the nitrogen molecule which has also shown the HF orbital wavefunction is sufficient to calculate the relativistic energy except from the spectroscopic work (58), but it still needs some Breit interaction type corrections and also some QED corrections as well.

4. CONCLUSION

The interaction in ten different conformers of pyrazine dimer have been investigated in terms of both supermolecular and DFT-SAPT approaches and doubly bridged structure was found as the global minimum on the potential energy surface. The cross displaced stacked dimer and T-shaped dimers have been determined as the most stable local minima respectively. Since CCSD(T) results were considered as our reference, MP2 and B3LYP-D overestimated the interaction energy while DFT-SAPT and SCS-MP2 make an underestimation. However, DFT-SAPT (LPBE0) results are the closest to CCSD(T) ones, thus it means the potential energy surface of pyrazine dimer can be treated with this method as an alternative to CCSD(T). Additionally, the only disadvantage of B3LYP-D appears in doubly bridged global minimum structure where the dispersion interaction is less important. When the basis set was increased from aug-cc-pVDZ to aug-cc-pVTZ, DFT-SAPT displayed the highest changes among all the methods.

For triazine, the global minimum is again found as the doubly-bridged conformer which is consistent with the crystal structure analysis results of the s-triazine. All the methods except MP2 have predicted the global minimum as the doubly-bridged conformer. It is important to see that the following most stable local minimum structures are mostly of stacked conformers which supports our previous qualitative predictions based on the electrostatic potential and polarizability arguments. Therefore, it may be concluded that diazines do not prefer a definite or general structural conformation, while triazines strongly prefer to be stacked in spatial configuration according to the orientational trend among the local minimum structures. Additionally, in diazines, the dominant interaction responsible for the crystal structure is the aromatic hydrogen bond, while in triazines, the dominant effect results from the classical hydrogen bond. Thus, one may expect to observe very different crsytal structures for diazines and triazines.

DFT-SAPT computations using LPBE0 functional give fairly good results close to CCSD(T) at almost all structures of triazine. Furthermore, SCS-MP2 was found as the second alternative method to CCSD(T) because of performing so well in numerous different structures better than the others methods. In the sense of computational cost, SCS-MP2 was found more suitable than DFT-SAPT (LPBE0) method to perform a potential energy surface scan to find a model potential necessary for a molecular dynamics simulation dealing with the crystallization process of both pyrazine and triazine.

B3LYP-D was found somewhat more favourable to use in treating the stacked structures where π-π interaction has the leading role depending highly on the dispersion interaction. It was also found that, B3LYP-D works quite well in T-shaped structures among the others. A highly remarkable result was found on the SAPT calculations. It may be concluded that, DFT-SAPT method has a vital functional dependence according to the difference between PBE0 and LPBE0 results.

By one-to-one comparison between similar structures of pyrazine and triazine, pyrazine conformers have slightly larger electrostatic and dispersion components than triazine although having smaller number of nitrogens. That causes from the fact that "number of hydrogens" is also important in the 1,2,3-N containing aromatic compound homolog series, not only "the number of nitrogens" is important.

The effect of relativistic corrections were found as negligible for these weak interactions in dimers, but vitally important for pyrazine and triazine monomers.

REFERENCES

[1] **Desiraju, G., Steiner, T.**, 1999. The Weak Hydrogen Bond, *Oxford Univ. Press*

[2] **Pauling, L.**, 1935: The Structure and Entropy of Ice and of Other Crystals with Some Randomness of Atomic Arrangement, *J. Am. Chem. Soc*., **57**, 2680.

[3] **Oki, M., Iwamura, H.**, 1959: Intramolecular Interaction between Hydroxyl Group and π-Electrons. II. Limitation of the Interaction by Chain-length in ω-Hydroxy-1-alkenes*Bull. of Chem. Soc. Japan*, **32**, 6, 567.

[4] **Pimentel, G: C.**, 1960. The Hydrogen Bond, *W. H. Freeman*, San Francisco.

[5] **McPhail, A. T., Sim, G: A.**, 1965: Interaction between phenol and various pi-bases. Preliminary infrared study, *Chem. Commun.*, 124.

[6] **Yoshida, Z., Osawa, E.**, 1965: Spectra and hydrogen bonding of diphenylcyclopropenone, *J. Am. Chem. Soc*., **87**, 1467.

[7] **Oki, M**. *et al*., 1968: Intramolecular interaction between a hydroxyl group and pi-electrons, *Tetrahedron*, **24**, 1905.

[8] **Perutz, M. F**. *et al*., 1986: Amino-aromatic interactions in proteins, *J. Am. Chem. Soc.*, **108**, 1064.

[9] **Nakatsu, S. K.**, *et al.*, 1978: 2,6-Diphenylphenol: a structure containing an intramolecular O-H$\cdots\pi$ hydrogen bond, *Acta Cryst., Sect. B*, 2357.

[10] **Aubry, A**., *et al*., 1977: Structure cristalline du tetraphenylborate de tributylammonium monohydrate: un exemple d'interaction H-pi, *Acta Crystallogr., Sect. B*, **33**, 2572.

[11] **Hardy, A: D. U., MacNicol, D.**, 1976: Crystal and molecular structure of an OH...π hydrogen-bonded system: 2,2-bis-(2-hydroxy-5-methyl-3-t-butylphenyl)propane, *J. Chem. Soc., Perkin Trans*., **2**, 1140.

[12] **Perutz, M.F., Levitt, M.**, 1988: Aromatic Rings Act as Hydrogen Bond acceptors, *J. Mol. Biol*., **201**, 751.

[13] **Dauster, I., Rice, C. A., Zielke, P.**, 2008: N-H...pi interactions in pyrroles: systematic trends from the vibrational spectroscopy of clusters, *Phys. Chem. Chem. Phys.*, **10**, 2827.

[14] **Busker, M., Haber, T., Kleinermanns, K.,** 2008: IR–UV double resonance spectra of pyrazine dimers: Competition between CH…π, π…πand CH…N interactions, *Chem. Phys. Lett*., **467**,251.

[15] **Tsuzuki, S., Honda, K**.; 2000: Origin of the Attraction and Directionality of the NH/π Interaction: Comparison with OH/π and CH/π Interactions, *J. Am. Chem. Soc*., **122**, 11450.

[16] **Emseis, P., Failes, T**., 2004: Structural sources of chiral discrimination in diastereoisomeric Ru(II) complexes of aromatic aminoacids and diimines, *Polyhedron*, **23**, 1749.

[17] **Stojonovic, S., Medokovic, V**., 2007: XH/p interactions with the pi system of porphyrin ring in porphyrin-containing proteins**,** *J. Biol. Inorg. Chem*., **12**, 1063.
[18] **Stone, A. J.**, 1997. The Theory of Intermolecular Forces, *Oxford Univ. Press*.
[19] **Kaplan, I. G.**, 2006. Intermolecular Forces, *Wiley & Sons*.
[20] **Pitzer, K.**, 1959: Intermolecular and intramolecular forces and molecular polarizability, *Adv. Chem. Phys*., **2**.
[21] **Scheiner, S.**, 1997. Hydrogen bonding, *Oxford Press*.
[22] **Brinkley, R.L., Gupta, R.B.**, 2001: Hydrogen bonding with aromatic rings, *Thermodynamics*, **47**, 948.
[23] **Rozas, I., Alkarta, I., Elguero, J**., 1997: Unusual Hydrogen Bonds, *J. Phys. Chem. A*, **101**, 9457.
[24] **Al-Juaid, S., Al-Nasr, A.., Eaborn,** 1991: Crystallographic evidence for intermolecular hydrogen bonding between aryl groups and OH groups in silanols, *J. Chem. Soc. Chem*., 1482.
[25] **Crisma, M., Formaggio, F.**, 1997: Experimental evidence at atomic resolution for intramolecular NH/π (Phenyl) interactions, *Biopolymers*, **42**, 1.
[26] **Broda, M., Siodlak, D., Rzeszotarska, B**., 2005: The effect of beta-methylation on the conformation of alpha, beta-dehydrophenylalanine: a DFT study, *J. Peptide Sci*.,**11**, 235.
[27] **Munoz, M. A., Sama, O.**, 2001: Hydrogen bonding NH/ π interactions between betacarboline and methyl benzene derivatives, *Spectrochimica Acta A*, **57**, 1049.
[28] **Stefov, V., Pejov, L.**, 2003: Experimental and quantum chemical study of pyrrole self-association through N–H· · ·p hydrogen bonding, *J. Mol. Struc*., **649**, 231.
[29] **Joachain, C., Bransden, H.**, 1999. Atom ve Molekül Fiziği, *Bilim Yay*. (çev.)
[30] **Dereli, T., Verçin, A.**, 2000. Kuantum Mekaniği I, *METU Press*.
[31] **Aygün, E., Zengin, M.**, 1993. Atom ve Molekül Fiziği, *Bilim Yay*.
[32] **Mortimer, R. G.**, 2000. Physical Chemistry, *Academic Press*.
[33] **Pilar, F.**, 2001. Elementary Quantum Chemistry, *Dover*.
[34] **Davis, J.**, 1965. Advanced Physical Chemistry, *Ronald Press*.
[35] **Wilson, E.**, 1996. Molecular Vibrations, *Dover*.
[36] **Hougen, J., Bunker, P., Johns, W**., 1970: The vibration-rotation problem in triatomic molecules allowing for a large-amplitude bending vibration, *J. Mol. Spec*., **34**, 136.
[37] **Spirko, V., Cejchan, A., Lutchyn, R**., 2002: Dimensionality of Proton Transfer in the Intramolecular Hydrogen Bond of Formimidol, *Chem. Phys. Lett*., **355**, 319.
[38] **Hobza, P., Spirko, V**., 2009: The structure and vibrational dynamics of the pyrrole dimer, *Phys. Chem. Chem. Phys*., **11**, 3885.
[39] **Tekin, A., Jansen, G**., 2007: How accurate is the density functional theory combined with symmetry-adapted perturbation theory approach for CH–pi and pi–pi interactions? A comparison to supermolecular calculations for the acetylene–benzene dimer, *Phys. Chem. Chem. Phys*., **9**, 1680.
[40] **Kim, S., Tarakeshwar, P., Lee, J.Y**., 2000: Molecular Clusters of π-Systems: Theoretical Studies of Structures, Spectra, and Origin of Interaction Energies, *Chem. Rev*., **100**, 4145.

[41] **Hartree, D. R.**, 1928: The Wave Mechanics of an Atom with a Non-Coulomb Central Field. Part I. Theory and Methods, *Proc. Cambridge Phil. Soc*., **24**, 89.
[42] **Fock, V.,** 1930: Näherungsmethode zur Lösung des quantenmechanischen Mehrkörperproblems, *Z. Physik*, **61**, 126.
[43] **Fock, V.**, 1974. Fundamentals of Quantum Mechanics, *Mir Pub*., Moscow.
[44] **Moser, C., Lefebvre, R., Daudel, R.**, 1959. Quantum Chemistry, *Interscience*.
[45] **Löwdin, P. O.**, 1959: Theory of electron correlation, *Adv. Chem. Phys*., **2**, 207.
[46] **Sinanoğlu, O.**, 1972. New Directions in Atomic Physics, *Yale Press*.
[47] **Szabo, A., Ostlund, N.**, 1996. Modern Quantum Chemistry, *Dover*.
[48] **Watson, R.**, 1960: Approximate Wave Functions for Atomic Be, *Phys. Rev*., **119**, 170.
[49] **Nesbet, R. K.**, 1967: Atomic Bethe-Goldstone Equations, *Phys. Rev*., **155**, 51.
[50] **Sinanoğlu, O.**, 1964: Many electron theory of atoms, molecules and their interactions, *Adv. Chem. Phys*., **6**, 315.
[51] **Sinanoğlu,O., Brueckner,K.**, 1970. Three Approaches to Electron Correlation, *Yale Press*.
[52] **Hill, T.**, 1987. Statistical Mechanics, *Dover*.
[53] **Hsu, K., Hosteny, R., Shavitt, I**., unpublished results (see. Ref. 47).
[54] **Wohl, A., Das, G.**, 1970: The method of optimized valence configurations, *Adv. Quant. Chem*., **5**, 261.
[55] **Goddard, W., Dunning, H., Hay, P.**, 1973: Generalized valence bond description of bonding in low-lying states of molecules, *Acc. Chem. Res*., **6**, 368.
[56] **Siegbahn, P.**, 1980: A Comparison of the Super-CI and the Newton-Raphson Scheme in the Complete Active Space SCF Method, *Phys. Scr*., **21**, 323.
[57] **Cizek, J.**, 1966: On the Correlation Problem in Atomic and Molecular Systems. Calculation of Wavefunction Components in Ursell-Type Expansion Using Quantum-Field Theoretical Methods, *J. Chem. Phys*., **45**, 4256.
[58] **Wilson, S.**, 2007. Electron Correlation in Molecules, *Dover*.
[59] **Brueckner, K. A**., 1955: Many-Body Problem for Strongly Interacting Particles. II. Linked Cluster Expansion, *Phys. Rev*., **100**, 36.
[60] **Moeller, C., Plesset, M. S.,** 1934: Note on an Approximation Treatment for Many-Electron Systems, *Phys. Rev*., **46**, 668.
[61] **Goldstone, J.**, 1957: Derivation of the Brueckner Many-Body Theory, *Proc. Roy. Soc*., **A239**, 267.
[62] **Roothaan, C. C. J.**, 1951: New Developments in Molecular Orbital Theory, *Rev. Mod. P*hys., **23**, 69.
[63] **Helgaker, T., Jorgensen,** 2000. Molecular Electronic Structure Theory, *Wiley*.
[64] **Piela, L.**, 2007. Ideas of Quantum Chemistry, *Elsevier*.
[65] **Bartlett, R. J., Hirata, S.**, 2000: A high performance ab initio electronic structure program package, *Chem. Phys. Lett*., **321**, 216.
[66] **Bartlett, R.**, 1985. Comparison of Ab Initio Quantum Chemistry with Experiment for Small Molecules, *D. Reidel Pub*.
[67] **Yarkony, D.**, 1995. Modern Electronic Structure Theory, *World Scientific*.
[68] **Dirac, P. A. M**., 1928: The Quantum Theory of the Electron, *Proc. Roy. Soc*., A117, **610**.
[69] **Dirac, P. A. M.**, 1928: The Quantum Theory of the Electron: Part II, *Proc. Roy.*

Soc., A118, **351**.
[70] **Dirac, P. A. M.**, 2007. The Principles of Quantum Mechanics, *Oxford Press*.
[71] **Sherwin, C.**, 1959. Introduction to Quantum Mechanics, *Rinehart & Winston*.
[72] **Messiah, A.**, 1999. Quantum Mechanics, *Dover*.
[73] **Merzbacher, E.**, 1970. Quantum Mechanics, *John Wiley & Sons*.
[74] **Schiff, L.**, 1949. Quantum Mechanics, *McGraw-Hill*.
[75] **Cohen-Tannoudji, C.,** 1977. Quantum Mechanics, *John Wiley & Sons*.
[76] **Pilkuhn, H.**, 2005. Relativistic Quantum Mechanics, *Springer-Verlag*.
[77] **Bethe, H., Salpeter,E.**, 1957. Quantum Mechanics of One- and Two-Electron Atoms, *Cornell Univ. Press*.
[78] **Reiher, M., Wolf, A.**, 2008. Relativistic Quantum Chemistry, *Wiley*.
[79] **Dyall, K., Knut Faegri, J.**, 2007. Introduction to Relativistic Quantum Chemistry, *Oxford*.
[80] **Pyykkö, P.**, 2000. Relativistic Theory of Atoms and Molecules, *Springer*.
[81] **Pitzer, K.**, 1979: Relativistic effects on chemical properties, *Acc. Chem. Res.*, **12**, 271.
[82] **Reiher, M., Wolf, A.**, 2004: Exact decoupling of the Dirac Hamiltonian. I. General Theory, *J. Chem. Phys.*, **121**, 2037.
[83] **Reiher, M., Wolf, A.**, 2004: Exact decoupling of the Dirac Hamiltonian. II. The generalized Douglas--Kroll--Hess transformation up to arbitrary order, *J. Chem. Phys.*, **121**, 10945.
[84] **Reiher, M., Wolf, A.**, 2006: Exact decoupling of the Dirac Hamiltonian. IV. Automated evaluation of molecular properties within the Douglas-Kroll-Hess theory up to arbitrary order, *J. Chem. Phys.*, **124**, 064103.
[85] **Reiher, M., Wolf, A.**, 2006: Exact decoupling of the Dirac Hamiltonian. III. Molecular properties, *J. Chem. Phys.*, **124**, 064102.
[86] **Craig, D., Thirunamachandran, T.**, 1998. Molecular Quantum Electrodynamics, *Dover*.
[87] **Veillard, A., Clementi, E.**, 1968: Correlation Energy in Atomic Systems. V. Degeneracy Effects for the Second-Row Atoms, *J. Chem. Phys.*, **49**, 2415.
[88] Advances in Chemical Physics, **Vol. 12**, Intermolecular Forces, 1967, *Interscience Wiley*.
[89] **Jeziorski, B.,** 1994: Perturbation Theory Approach to Intermolecular Potential Energy Surfaces of van der Waals Complexes, *Chem. Rev.*, **94**, 1887.
[90] Handbook of Mol. Phys. and Quant. Chem., **Vol. 3**, Ed. by S. Wilson, 2003, *John Wiley*.
[91] **Grimme, S.**, 2003: Improved second-order Møller-Plesset perturbation theory, *J. Comp. Chem.*, **24**, 13, 1529.
[92] **Jansen, G., Heßelmann, A.**, 2001: Comment on "Using Kohn−Sham Orbitals in Symmetry-Adapted Perturbation Theory To Investigate Intermolecular Interactions, *J. Phys. Chem. A*, **105**, 11156.
[93] **Heßelmann, A., Jansen, G.**, 2002: First-order intermolecular interaction energies from Kohn–Sham orbitals, *Chem. Phys. Lett.*, **357**, 464.
[94] **Heßelmann, A., Jansen, G.**, 2002: Intermolecular induction and exchange-induction energies from coupled-perturbed Kohn–Sham density functional theory, *Chem. Phys. Lett.*, **362**, 319.
[95] **Heßelmann, A., Jansen, G**., 2003: Intermolecular dispersion energies from

time-dependent density functional theory, *Chem. Phys. Lett*., **367**, 778.
[96] **Podeszwa,R., Jeziorski,B., Szalewicz,K**., 2005: Accurate interaction energies for argon, krypton, and benzene dimers from perturbation theory based on the Kohn–Sham model, *J.Chem.Phys*., **123**, 214103.
[97] **Jansen, G., Heßelmann, A., Schutz, M.**, 2005: Density-functional theory-symmetry-adapted intermolecular perturbation theory with density fitting: A new efficient method to study intermolecular interaction energies, *J. Chem. Phys*.,**122**, 014103.
[98] **Jørgensen,P., Helgaker,T.**, 1996: Modern electronic structure theory, *Chem. Phys. Lett*., 263,**3**,530.
[99] **Feyereisen, M.; Fitzgerald, G.,** 1993: Use of approximate integrals in ab initio theory. An application in MP2 energy calculations, *Chem. Phys. Lett*., 208, 5, **6**, 359.
[100] **Kendall, R.A., Früchtl, H.A.**, 1997: The impact of the resolution of the identity approximate integral method on modern ab initio algorithm development, *Theor. Chem. Acc*., **97**, 158.
[101] **Wheatley, P.J.**, 1957: The crystal structure of pyrazine, *Acta Cryst*.,**10**, 182.
[102] **Thalladi, V., Boese, R., Gehrke, A.**, 2000: Crystal Engineering with -CH···N and =CH···N Hydrogen Bonds, *New J. Chem*., **24**, 463.
[103] **Mishra, B.K.**, 2006: Van der Waals Complexes of Small Molecules with Benzenoid Rings, *J. Theor. Comp. Chem*.,5, **3**, 609.
[104] **Prasad, S.M.**, *et.al*., 1981: The crystal structure of s-triazine at 5K, *J. Phys. Chem.:Solid State Phys*.,**14**, L929.
[105] **Smith, J., Rae, A.**, 1978: Effect of neutron irradiation on the density of low-energy excitations in vitreous silica, *J. Phys. Chem.:Solid State Phys*., **11,** 347.
[106] MOLPRO 2009.1.
[107] TURBOMOLE 6.0.
[108] PHYTHON 2.4.1.

APPENDIX

An example of the MOLPRO script, prepared for the CCSD(T) calculation with aug-cc-pVDZ basis including CP correction:

```
---------------------------------------------------------------------------------------------------
memory,170,m
gthresh,energy=1d-8,orbital=1d-7
basis=avdz
symmetry,z
angstrom
GEOMTERY={
N1,,     3.9771614,    1.3681646,    0.0000000
N2,,     1.1282201,    1.5371430,    0.0000000
C1,,     3.1856070,    0.2728176,    0.0000000
C2,,     1.7801251,    0.3502321,    0.0000000
C3,,     1.9182699,    2.6339436,    0.0000000
C4,,     3.3221396,    2.5501680,    0.0000000
H1,,     3.6892505,   -0.6989177,    0.0000000
H2,,     1.1603478,   -0.5532410,    0.0000000
H3,,     1.4158720,    3.6064677,    0.0000000
H4,,     3.9365218,    3.4560481,    0.0000000
N3,,    -1.1282206,   -1.5371554,    0.0000000
N4,,    -3.9771608,   -1.3681521,    0.0000000
C5,,    -1.9182804,   -2.6339490,    0.0000000
C6,,    -1.7801153,   -0.3502389,    0.0000000
C7,,    -3.1855965,   -0.2728122,    0.0000000
C8,,    -3.3221494,   -2.5501611,    0.0000000
H5,,    -1.4158912,   -3.6064778,    0.0000000
H6,,    -1.1603302,    0.5532288,    0.0000000
H7,,    -3.6892314,    0.6989277,    0.0000000
H8,,    -3.9365394,   -3.4560358,    0.0000000
}
int
! --- dimer ---
hf
e_dim_hf=energy
ccsd(t)
e_dim_mp2=emp2
e_dim_ccsd=energc
e_dim_ccsdt=energt(1)
! --- monomerA-CP  ---
dummy,N3,N4,C5,C6,C7,C8,H5,H6,H7,H8
```

```
hf
e_mA_CP_hf=energy
ccsd(t)
e_mA_CP_mp2=emp2
e_mA_CP_ccsd=energc
e_mA_CP_ccsdt=energt(1)
! --- monomerB-CP  ---
dummy,N1,N2,C1,C2,C3,C4,H1,H2,H3,H4
hf
e_mB_CP_hf=energy
ccsd(t)
e_mB_CP_mp2=emp2
e_mB_CP_ccsd=energc
e_mB_CP_ccsdt=energt(1)
e_int_hf = e_dim_hf - e_mA_CP_hf - e_mB_CP_hf
e_int_mp2 = e_dim_mp2 - e_mA_CP_mp2 - e_mB_CP_mp2
e_int_ccsd=e_dim_ccsd-e_mA_CP_ccsd-e_mB_CP_ccsd
e_int_ccsdt=e_dim_ccsdt-e_mA_CP_ccsdt-e_mB_CP_ccsdt
```

BIOGRAPHY

Candidate's full name:	Berkay SÜTAY
Place and date of birth:	Istanbul, 08.07.1986
Permanent Address:	Sancaktar Tekke Sok. Dilek Apt. No:3/6 Kocamustafapaşa - Istanbul TÜRKİYE
Universities and Colleges attended:	High School Graduate, Şehremini High School (2005) B.Sc. Degree, Yıldız Technical University, Faculty of Art&Science, Chemistry Department (2005-2009). M.Sc. Degree, Istanbul Technical University, Institute of Science and Technology, Chemistry Department (2009-2010)